Review

Israel Journal of Chemistry

doi.org/10.1002/ijch.202100073

Metal-Organic Frameworks as a New Platform for Enantioselective Separations

Gaurav Verma[+],[a] Ruhi Mehta[+],[b] Sanjay Kumar,*[b] and Shengqian Ma*[a]

Abstract: The enantioselective separation of racemic mixtures is highly important in the pharmaceutical, food and agrochemical sector. Metal-organic frameworks, as a class of highly porous materials are emerging as highly efficient and selective platforms for chiral recognition and separation owing to their ultrahigh porosities, functionalized pore walls, controllable pore chemistry and presence of highly ordered chiral recognition sites. In this review, we summarize the progress made in the synthesis of chiral MOFs via direct and indirect methods, followed by their applications in some important chiral separations of alcohols, drugs, amino acids, biologically relevant molecules and important chiral organic mixtures. The developments in chiral MOF membranes as thin films for practical industrial use are also explored. Finally, the outlook for the MOFs as emerging platforms for enantioseparation and the future directions are discussed.

Keywords: metal-organic frameworks · chiral · enantioselective separation · membrane · thin-film

1. Introduction

Chirality plays a crucial role in the evolution of life as it forms the basis of various essential elements of biological systems such as proteins, nucleic acids, amino acids, sugars and various nucleosides which are the basic building blocks of all living beings. The concept of optical rotation has been known since 1848 when Pasteur attained crystals of sodium ammonium tartrate and studied their optional rotations.[1]

Even though the concept of optical rotation was already established; the term "chirality" was proposed 45 years later by Lord Kelvin. Chirality/handedness describes the molecular asymmetry, i.e. a molecule having no center or plane of symmetry.[2] Molecular chirality is often followed by enantiomerism; whereby the non-superimposable mirror images of chiral molecules form pairs of enantiomers with identical physical properties but different orientation/arrangement of the atoms.[3] This trivial alteration in the arrangement of atoms changes the biological properties of the molecule and plays a vital role in various pharmaceutical, agrochemical and food industries.[4]

The action of drugs on human body is dependent on chirality matching with the target molecules. The drug racemate generally has only one enantiomer which proves out to be effective (called eutomer) whereas the other enantiomer can either be non-effective (called distomer) or even toxic. For instance, the R-enantiomer of thalidomide is a sedative given to pregnant women, whereas the S-enantiomer of the drug can cause fetal abnormalities.[5] Hence, focus on single-enantiomeric drug development becomes vital and has pushed the researchers and chemists to develop new methods to separate the enantiomers.

Apart from various conventional enantio-separation strategies such as kinetic resolution, chemical resolution, membrane resolution, asymmetric synthesis, chromatographic techniques and catalytic separation, various new strategies have also been adopted to obtain single enantiomer. These methodologies have focused on the development of chiral selector (SO) molecules, however they lead to high cost, low yields as well as huge time-consumption.[6]

Amongst all these techniques, chromatography is the most efficient and advantageous method for enantioseparation and numerous chiral stationary phases (CSPs) have been prepared from chiral selectors; and categorized into polymers, CD (cyclodextrins), proteins, antibiotics, Pirkle type etc. These have been further used in various analytical and preparative techniques like high-performance liquid chromatography (HPLC), gas chromatography (GC), capillary electrochromatography (CEC), thin layer chromatography (TLC), stimulated moving bed (SMB) and supercritical fluid chromatography (SFC).[3,7] However, liquid chromatography (LC) and gas chromatography are the widely exploited analytical techniques for enatioseparation.[8] Despite such myriad techniques available for enantiomeric resolution, the separation of the enantiomeric pairs with high efficacy is challenging due to high cost, low versatility, poor recovery and moderate efficiencies.

[a] *G. Verma,[+] S. Ma*
Department of Chemistry,
University of North Texas,
1508 W Mulberry St, Denton, TX 76201, USA
Phone: 1-940-369-7137
E-mail: Shengqian.Ma@unt.edu
[b] *R. Mehta,[+] S. Kumar*
Department of Chemistry,
Multani Mal Modi College,
Patiala 147001, Punjab, India
E-mail: sanjay2002@gmail.com
[+] *Both authors contributed equally to this work.*

Since the last few decades, porous materials having permanent porosities have attracted widespread attention owing to their capability to selectively trap one of the enantiomer (guest molecule) from a racemic mixture while retaining their structure after removal of the guest fragment. The solid porous crystalline materials can be categorized into: 1) organic frameworks such as hydrogen-bonded organic frameworks (HOFs) and covalent organic frameworks (COFs) 2) inorganic networks such as aluminosilicate zeolites and 3) organic-inorganic hybrid materials such as metal-organic frameworks (MOFs).[9] Aluminosilicate zeolites (general formula $M_{x/n}{}^{n+}[(AlO_2)_x(SiO_2)_y]^{x-}$) have been extensively used for development of different chiral separators,[10] but lack an extensive use due to their cumbersome methods of preparation and low structural diversity.[11] The MOFs, COFs and HOFs on the other hand show tunability by virtue of design, richness of structural architectures, ease of preparation and better structural properties.

MOFs or porous coordination polymers (PCPs) are a class of diverse structures with pleasing architectures which have been known since 1999 when MOF-5 (based on $Zn_4O(CO_2)_6$ octahedral secondary building units (SBUs) linked with 1,4-benzenedicarboxylate (bdc)) was first synthesized by Yaghi et al.[12] Since then, through reticular chemistry a wide variety of MOFs have been designed and formulated by linking organic fragments such as: carboxylate, azolate, pyrazolate, imidazolate etc. with metal ion/ clusters. MOF are known for their exceptionally high surface areas, pore sizes and rigid structural integrities.[13]

MOFs having different pore/cavity sizes for variety of applications including fluorescence sensing, gas storage and separation, proton and electron conduction, catalysis, drug delivery and environmental remediation have been developed.[14] Owing to their porous architectures, chemical/ structural flexibility, tailorability and inclusion of various functionalities by structural or post-synthetic modifications; MOFs show tremendous potential to separate enantiomers which is very crucial in the preparation of biologically and pharmacologically essential molecules.

Although the chiral metal organic materials had been around for some time,[15] the first application of chiral MOFs in enantioseparation was carried out by Kim et al. in 2000 to separate the racemic isomers of $[Ru(2,2'\text{-bpy})_3]^{2+}$ (bpy: bipyridine) with 66% ee using homochiral POST-1 (POST: Pohang University of Science and Technology).[16] Since then, the research in this area has shown tremendous growth (Figure 1) and continues to flourish for targeting custom chiral separation applications. The increasing importance of this field can be further realized by the burgeoning number of critical reviews emerging in the literature,[9b,c,17] highlighting the importance of chiral MOFs and their versatility in chiral catalysis and separations. MOFs have been employed for separating a variety of racemic mixtures, developed as CSPs for HPLC, LC, GC; and processed into membranes and chiral columns. However, a more comprehensive overview of the advancements in the synthesis strategies with a critical examination of each approach is needed for a better and judicious design of the chiral MOFs. Furthermore, as we move

Gaurav Verma obtained his Ph.D. from the University of South Florida in 2020 under the supervision of Prof. Shengqian Ma. Currently he is working as a Postdoctoral Research Fellow in the group of Prof. Shengqian Ma at the University of North Texas. His areas of interest include design and synthesis of MOFs for energy, catalysis and separation applications.

Ruhi Mehta received her Master's in Chemistry (M.Sc.) in 2011 from Punjabi University, Patiala, India. She did her Ph.D. from Thapar Institute of Engineering and Technology, Patiala, India. Her research areas of interest are in studying the photophysical properties of different supramolecules and applications of porous materials in organic separations. She is presently working as Assistant Professor in the Dept. of Chemistry at Multani Mal Modi College, Patiala, India.

Sanjay Kumar obtained his Ph.D degree from Punjabi University, Patiala, India and worked as a UGC Raman Postdoctoral Fellow with Prof. Shengqian Ma from November 2014 to March 2016 at the University of South Florida. He is currently working as an Assistant Professor in Chemistry at Multani Mal Modi College, Patiala, India. His research interests include synthetic organic chemistry, porous materials with a focus on design and synthesis of MOFs, and the applications of MOFs for catalysis, separation, and gas storage.

Prof. Shengqian Ma obtained his B.S. degree from Jilin University, China in 2003, and graduated from Miami University (Ohio) with a Ph.D. degree under the supervision of Hong-Cai Joe Zhou (currently at Texas A&M University) in 2008. After finishing two-year Director's Postdoctoral Fellowship at Argonne National Laboratory, he joined the Department of Chemistry at University of South Florida (USF) as an Assistant Professor in August 2010. He was promoted to an Associate Professor with early tenure in 2015 and to a Full Professor in 2018. In August 2020, he joined the Department of Chemistry at University of North Texas (UNT) as the Robert A. Welch Chair in Chemistry.

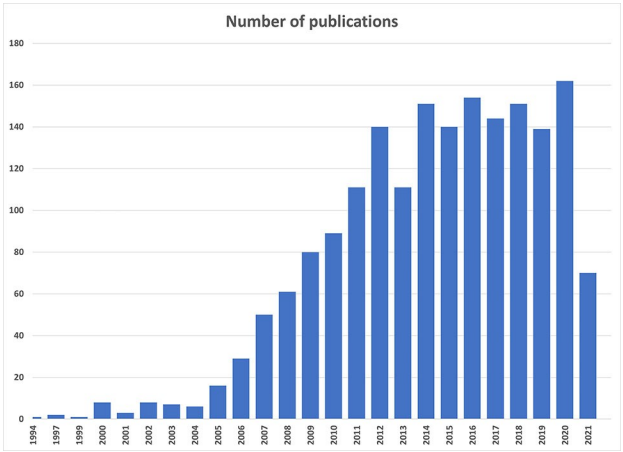

Figure 1. Growth in the number of publications on chiral metal organic frameworks over the past two decades. Adapted from Web of Science search on frameworks reported with the terms "chiral metal-organic frameworks" in all databases from 1994 to 2020.

towards more pragmatic applications of the chiral MOFs, an inspection of the progress towards processing them into membranes and thin films is needed.[17a,c,f,j,l,m,18]

In this contribution, we aim at providing an overview of the developments in the synthesis strategies for the chiral MOFs and their applications in enantioselective separations of racemic mixtures. Firstly, the direct and indirect methods for the design and synthesis of the chiral MOFs are discussed in detail outlining the assets and shortcomings of each strategy. Also, we have followed a different approach for the classification of the chiral MOF preparation methods. Any method that generates the chiral MOF from direct synthesis is clasified as a "direct method". Any other strategy that follows use of extrenal agents of post-modification is termed as "indirect method". This is followed by an elaborative examination of the applications of the chiral MOFs in enantioseparation of various types of racemic mixtures. Then, the developments of MOFs as membranes and thin-films for pragmatic applications are summarized to provide a future direction of these chiral MOFs in their practical use. Many excellent reviews have covered the use of MOFs as chiral stationary phases in chromatography and it is beyond the scope of this review, so it has not been covered here. Finally, the perspectives of the MOFs as platforms for enantioselective separations, and the challenges faced ahead are briefly discussed.

2. Chiral MOFs and their Synthesis Strategies

The chiral MOFs are coming to the fore due to their applicability in different fields such as molecular recognition, asymmetric catalysis, enantioseparation and non-linear optics.[17a,h,18a,b,19] This wide scale applicability of chiral MOFs can be attributed to their porosity, adsorption capacity, large internal surface area, stabilities, structural integrity and most importantly their chiral environment for recognition of specific enantiomer (guest).

The biggest merit manifested in the chiral MOF systems is the integration of the advantages of heterogeneous catalysts such as high stability, recyclability, ease of separation, high recovery of the catalyst and low cost; as well as those of homogeneous catalysts like high efficiency, selectivity, homogeneous active sites and milder reaction conditions. Introduction of chirality into the final rigid microporous MOF by following different strategies has led to the development of frameworks with highly selective enantiomeric separation capabilities.[17e,g–i,k]

The construction of chiral MOFs from different metal ions/clusters and organic linkers can be categorized into two main strategies: (a) direct methods involving the use of chiral ligands, and (b) indirect methods consisting of post-synthetic modification, superficial chiral etching, chiral induction from achiral precursors, and chiral resolution (Scheme 1). The direct methods provide bulk homochirality, versatility, uniform active sites, very high activities and enantioselectivities; but suffer from the disadvantages of tedious synthesis and the need for high purity expensive reagents. The indirect methods on the other hand offer: use of achiral precursors which are cheap and readily available, flexibility to introduce different functional groups, and large-scale applicability; however, there are also certain drawbacks such as limited control of desired chirality, exhaustive design process, possibility of racemic mixtures and indiscriminate catalytic sites.

Both strategies have been extensively utilized and the selection of the optimal method varies depending on the system and the type of targeted applications. Representative examples of these different approaches used to construct the chiral MOFs are discussed in the following sections.

2.1 Direct Methods

2.1.1 Chiral MOFs from Chiral Fragments

This is the most common and efficient strategy for the direct construction of chiral MOFs in one-pot by using chiral monomers/building blocks. It ensures bulk homochirality of the resultant framework and generates intriguing architectures with high reliability. For instance, the homochiral D-POST-1 $[Zn_3(\mu_3\text{-}O)(L^1)_6]\cdot 2H_3O\cdot 12H_2O$ (L^1: 2,2-Dimethyl-5-[(4-

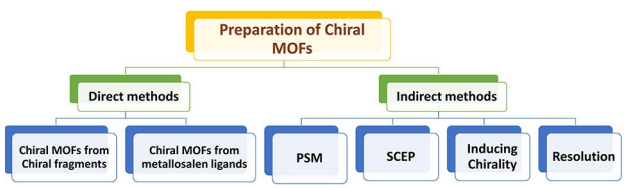

Scheme 1. The synthetic strategies for the preparation of chiral MOFs by direct and indirect methods.

pyridinylamino)carbonyl]-1,3-dioxolane -4-carboxylic acid), mentioned earlier was synthesized from a chiral bridging ligand derived from D-tartaric acid and Zn^{2+} ions. Even the L-POST-1 could also be prepared by reaction of the L-tartaric acid and Zn^{2+} employing the same reaction conditions.[16] Various other chiral linkers such as camphoric acid, amino acids and their derivatives, 2,2'-bis (diphenylphosphino)-1,1'-binaphthyl (BINAP) based linkers, diamine and diacids (Scheme 2) have been used to introduce chirality into the MOF systems.

Camphoric acid is an important linker used in the design and synthesis of the chiral MOFs. In 2008, Zhang and co-workers prepared six novel series of 3D chiral open and intrinsic-frameworks: (TMA)[In(D-cam)$_2$]·2H$_2$O, (TMA)[In-(L-cam)$_2$]·2H$_2$O, (choline)[In(D-cam)$_2$]·2H$_2$O, Co(D-cam)$_{1/2}$(bdc)$_{1/2}$(tmdpy), Ni(D-cam)(H$_2$O)$_2$ and [Mg(L-ma)(H$_2$O)$_2$]·(H$_2$O) (tmdpy: 4,4'-trimethylenedipyridine, D-cam: D-camphoric acid, L-cam: L-camphoric acid, L-ma: L-malic acid, and TMA: trimethylamine). Apart from the intrinsic chirality in the framework, these MOFs showed unusual chiral molecular integrity and helicity (controlled by the chiral building blocks).[20]

A novel homochiral MOF family was created by Zhao and co-workers by using RR-cam and SS-cam ligands, which displayed excellent structural, compositional, and chiral features. The CPM-311 through CPM-317 families (CPM: Crystalline Porous Materials) of the chiral MOFs comprised of all four RS-, SR-, RR-, and SS-homochiral forms. The inorganic chains adopted a 3_2 helix for RS-cam or RR-cam, whereas for the SR-cam or SS-cam a 3_1 helix is formed indicating that the stereochemistry around C1 of camphorates plays a very important role in determining the absolute helicity of chain (Figure 2). All the MOFs were diastereomeric as well as enantiomeric that enabled chiral-switching in these isoreticular frameworks. The chiral components showed versatility acting either as a cross-linker or an auxiliary ligand. This work provided a new vision for development of cost-effective yet valuable homochiral MOFs.[21]

The use of pillaring linkers along with the chiral linkers is another strategy to control the pore size and selectivity of the resultant MOFs. A helical and layered homochiral MOF [Zn$_2$(D-cam)$_2$(4,4'-bpy)]$_n$ was prepared by Yuan and co-workers whereby the layers of the MOF were pillared by the bipyridine fragments leading to the formation of two types of 3D self-penetrating structures. The homochiral framework consists of ordered left- and right-handed helical chains. The

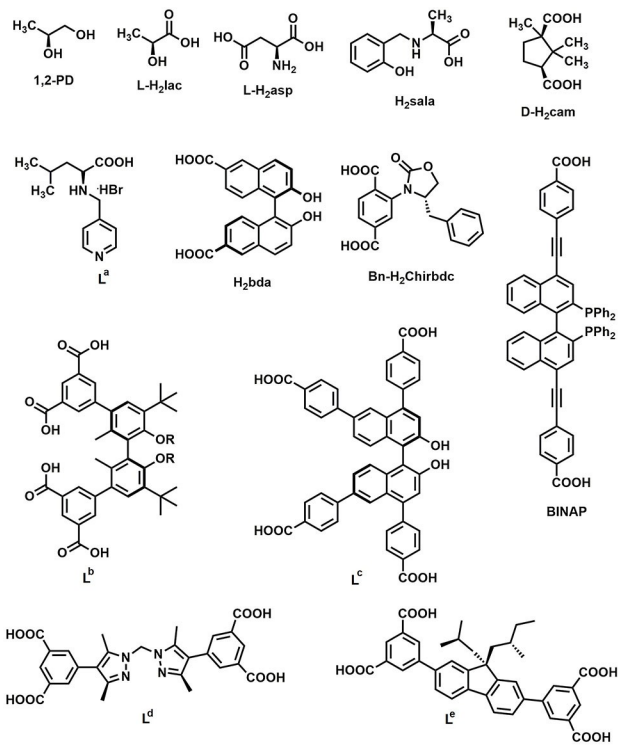

Scheme 2. Representative examples of chiral ligands for the construction of MOFs. (1,2-PD = 1,2-propanediol; L-H$_2$lac = L-lactic acid, L-H$_2$asp = L-aspartic acid, H$_2$sala = *N*-(2-hydroxybenzyl)-L-alanine, D-H$_2$cam = D-camphoric acid, H$_2$bda = 2,2′-hydroxy-1,1′-binaphthalene-6,6′-dicarboxylic acid, Bn-H$_2$Chirbdc: (S)-2-(4-Benzyl-2-oxooxazolidin-3-yl)terephthalic acid, BINAP: 2,2'-bis (diphenylphosphino)-1,1'-binaphthyl, L^a = N-(4-pyridylmethyl)-L-leucine·HBr, L^b = 3,3'-di-tert-butyl-5,5'-di(3,5-carboxyphenyl-1yl)-6,6'-dimethylbiphenyl-2,2'-dialkoxy linker, L^c = (R)-2,2'-dihydroxy-1,1'-binaphthyl-4,4',6,6'-tetrakis(4-benzoic acid), L^d = bis[4-(3,5-dicarboxyphenyl)-1H-3,5-dimethylpyrazolyl] methane, and L^e = 5,5′-(9,9-bis((S)-2-methylbutyl)-9H-fluorene-2,7-diyl)diisophthalic acid).

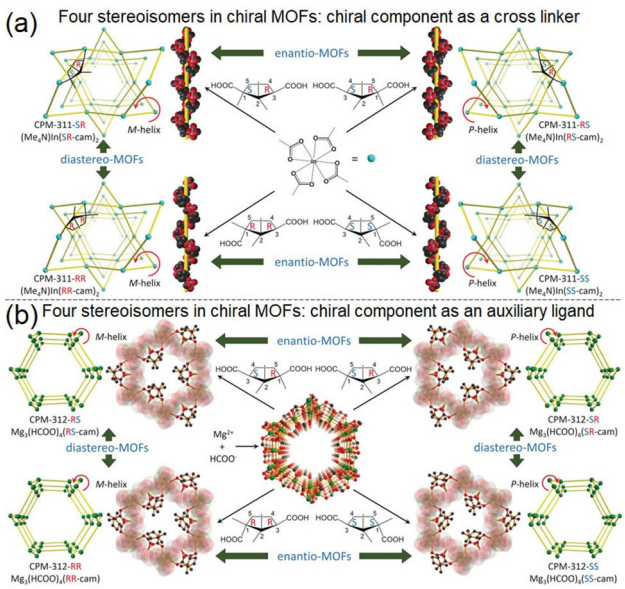

Figure 2. Chirality switching without topological change illustrated by two types of stereoisomerization in MOFs: (a) in CPM-311, the crystallization between the monomeric In(COO)$_4$ and four stereoisomers of camphoric acid leads to the same quartz type structure, and (b) in CPM-312, the crystallization between magnesium and formate form a honeycomb structure, with camphoric acid as a chiral pendant on the wall. Reproduced from Ref. 21 with the permission of John Wiley and Sons.

$[Zn_2(D\text{-}cam)_2(4,4'\text{-}bpy)]_n$ due to its high surface area, outstanding stability and ideal particle size with uniform shape distribution was further used for enantioseparation of nine

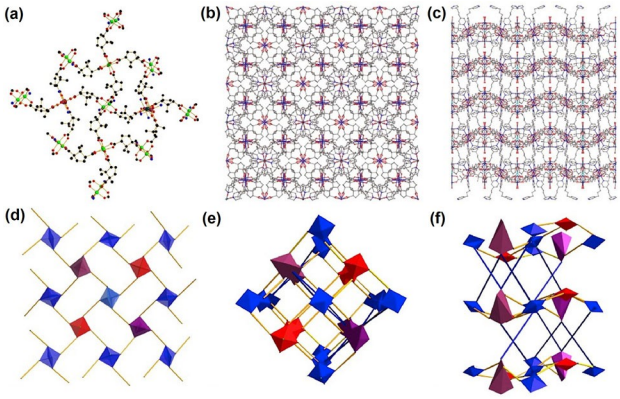

Figure 3. (a) Two-dimensional structure of $[Cu_6(D\text{-}cam)_8(TMDPY)_4Cd_2Na(OH)_4]$, (b) structure observed along the c-axis, (c) structure observed along the b-axis, (d) a simplified two-dimensional structure of the framework, (e) simplified three-dimensional structure observed along the c-axis, and (f) simplified structure observed along the b-axis. Cu_O: red polyhedron, Cu_N: blue polyhedron, Cd_{Na}: purple polyhedron, D-camphoric acid: yellow line, and TMDPY: blue line. Reproduced from Ref. 23 with the permission of Elsevier.

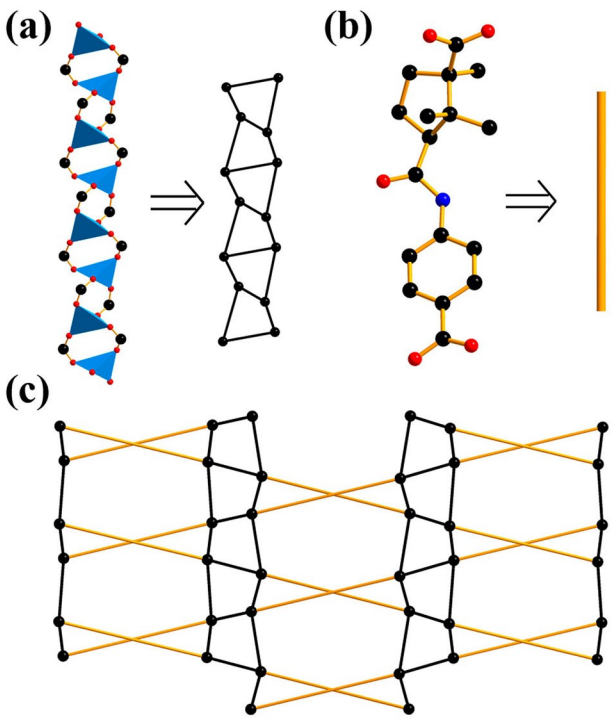

Figure 4. (a) Rod-shaped secondary SBU with polyhedral Zn simplified as a twisted ladder, (b) the ligand CTBA is considered as a stick, and (c) the net of the 2-dimensional layered framework. Reproduced from Ref. 24 with the permission of MDPI.

racemic mixtures of alcohol, aldehyde, phenol, base, amide, ketone and a drug via HPLC due to its low column pressure and excellent selectivity.[22]

Wang et al. also utilized TMDPY to connect the two dimensional structure formed by D-cam and copper clusters, giving rise to the three dimensional MOF $[Cu_6(D\text{-}cam)_8(TMDPY)_4Cd_2Na(OH)_4]$ (Figure 3). The synthesised material was further used for the separation of D/L-phenylalanine whereby the sorption of D-phenylalanine was relatively higher than L-phenylalanine.[23]

JUC-112, a 2D MOF based on rod-shaped Zn(II) SBUs and a chiral camphoric acid derivative, 4-(3-carboxy-2,2,3-trimethylcyclopentanecarboxamido)benzoic acid (H_2CTBA) was reported by Cai et al. (Figure 4). The extended multifunctional linker bestowed the framework with diverse applications in photoluminescence, water-alcohol separation and non-linear optics.[24]

The amino acids are the most prevalent chiral linkers occurring naturally. They offer a platform to generate a diverse array of structures through modification of the R group attached to the chiral center or by functionalization on the carboxyl and the amino groups. Furthermore, enantiopure chiral frameworks can be obtained from the naturally existing L or D configurations, respectively. Jacobson and co-workers obtained an optically pure one-dimensional network $[Ni_2O(L\text{-}Asp)(H_2O)_2]\cdot 4H_2O$ based on L-aspartic acid with extended Ni-O-Ni bonding under hydrolysis-favoring synthesis conditions.[25] Interestingly, upon increasing the pH from 5 to 7.2 under the same synthesis conditions, a 3D nickel aspartate MOF $[Ni_{2.5}(OH)(L\text{-}Asp)_2]\cdot 6.55H_2O$ with the same one-dimensional helical chains as found in $[Ni_2O(L\text{-}Asp)(H_2O)_2]\cdot 4H_2O$ was formed (Figure 5). The $[NiAsp_2]_2$ units link the 1D helical chains with the aspartate ligand in the tridentate chelating coordination mode. This work demonstrated the prospects of obtaining a myriad of frameworks from the same starting amino acid by tuning the pH of the environment.[26]

The frameworks of hard metal cations (e.g. Al^{3+}, Fe^{3+}, Zr^{4+}) with amino acids are relatively rare in the literature. In

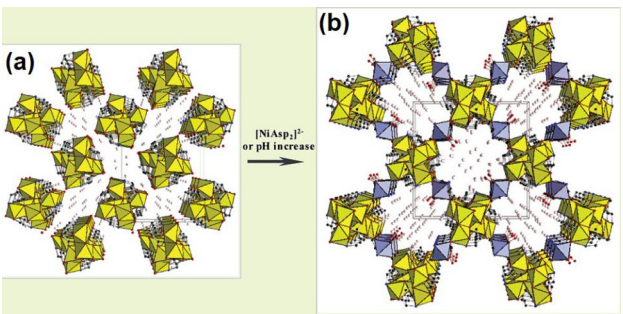

Figure 5. Crystal structures of (a) one-dimensional nickel aspartate $[Ni_2O(L\text{-}Asp)(H_2O)_2]\cdot 4H_2O$, and (b) the title three-dimensional material $[Ni_{2.5}(OH)(L\text{-}Asp)_2]\cdot 6.55H_2O$ formed by connecting chains in (a) through $[NiAsp_2]^{2-}$ bridges (shown as blue octahedra). Reproduced from Ref. 26 with permission of American Chemical Society.

2018, Serre and co-workers reported the 3D microporous MIP-202(Zr) (MIP: the Materials of the Institute of porous materials from Paris) constructed from 12-connected $Zr_6(\mu_3\text{-}O)_4(\mu_3\text{-}OH)_4$ node and the L-aspartate linker having a UiO-66 (UiO: Universitetet i Oslo) type structure (Figure 6). The MIP-202(Zr) showed good hydrolytic and chemical stability, even under varying pH environments (0 to 12) and in boiling water. Moreover, the material was synthesized in water thus featuring a green, scalable and cost-effective preparation of robust chiral MOFs using amino acids.[27]

An amino acid derived ligand 2,2′-(terephthaloyl bis-(azanediyl))bis(3-phenyl propanoic acid) (L^2) with C_2 symmetry, prepared from the condensation of (R)-/(S)-phenylalanine methyl ester and terephthaloyl chloride was used to construct

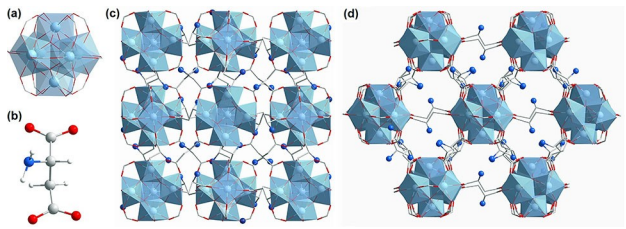

Figure 6. Crystal structural features of MIP-202(Zr): (a) the 12-connected $Zr_6(\mu_3\text{-}O)_4(\mu_3\text{-}OH)_4(COO-)_{12}$ cluster SBU, (b) an aspartic acid linker, (c) the crystal structure of MIP-202(Zr) viewed along the a-axis, and (d) the crystal structure of MIP-202(Zr) viewed along the (101) plane. Reproduced from Ref. 27 with the permission of Nature Publishing Group.

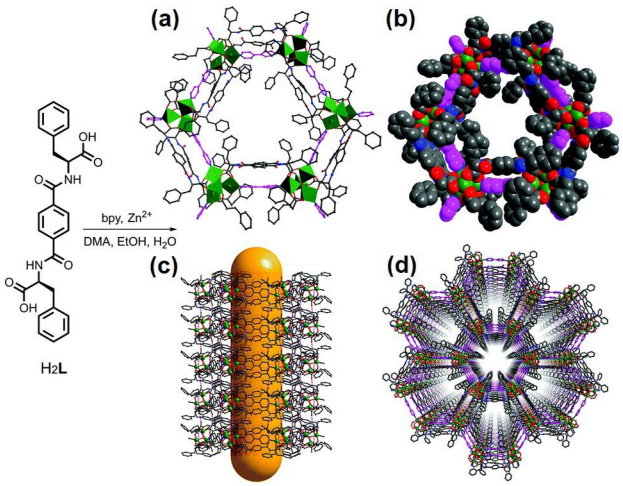

Figure 7. The synthesis of $[(Zn_4O)(L^2)_6(bpy)_3]$ and view of its structure: (a) the connection of Zn_4O clusters with L^2 ligands and bpy molecules generating a hexagonal window on the ab plane (green, Zn; grey, C; blue, N; red, O; bpy is highlight as purple), (b) illustration of the space-filling model of the open window along the *c*-axis, (c) the 1D nanotube highlighted as a yellow stick generated from the interlayer hydrogen-bonding along the *b*-axis, and (d) packing of the 3D supramolecular structure of $[(Zn_4O)(L^2)_6(bpy)_3]$. Reproduced from Ref. 28 with the permission of the Royal Society of Chemistry.

the chiral-MOF $[(Zn_4O)(L^2)_6(bpy)_3]$. The framework featured open-amphiphilic channels (Figure 7) deploying functionalized sites in form of hydrophilic amide groups and hydrophobic benzyl groups to modulate the interactions with the chiral adsorbate species. This allowed the MOF to exhibit excellent enantioseparation abilities for a variety of guests such as racemic secondary alcohols, epoxides, and ibuprofen; making it a promising potential stationary phase material.[28]

Yue et al. also prepared an enantiopure alanine derivative pyridine-2,6-dicarbonyl-bis(L-alanine) (H_2PDBAla) by functionalizing the amine group with pyridine-2,6-dicarboxylate; embedding features such as chirality, multifunctionality in the form of -C=O and -NH groups, and a V-shaped coordination configuration on the linker. The resultant chiral MOFs: $[Cu(PDBAla)(bpy)(H_2O)_2]\cdot 3H_2O$, $[Co(PDBAla)(bpy)(H_2O)_2]\cdot 3H_2O$ and $[Cu(PDBAla)(bpea)]\cdot 7H_2O$; (bpea = 1,2-bis(4-pyridyl)ethane)) displayed fascinating architectures with various topologies based on the right-handed helices and the ancillary N-donor ligands (Figure 8). The isostructural MOFs: $[Cu(PDBAla)(bpy)(H_2O)_2]\cdot 3H_2O$ and $[Co(PDBAla)(bpy)(H_2O)_2]\cdot 3H_2O$ contained a 2-fold interpenetrated 3D network with $CdSO_4$ (**cds**) topology, whereas in the third MOF **tcj** topology was observed. The materials showed good CO_2 adsorption performance and the $[Cu(PDBAla)(bpea)]\cdot 7H_2O$ was further used for enantioselective separation of alcohols.[29]

More recently, Zaworotko and coworkers utilized the linker R/S-mandelate to generate a family of 4th generation chiral MOFs having rigid framework and flexible/adaptable pores; derived from the previously reported parent structure $[Co_2(S\text{-mandelate})_2(4,4'\text{-bipyridine})_3](NO_3)_2$ (CMOM-1S/R; CMOM: chiral metal-organic materials) in order to elucidate the mechanism of chiral selectivity in porous materials by altering through host-guest or guest-guest interactions using

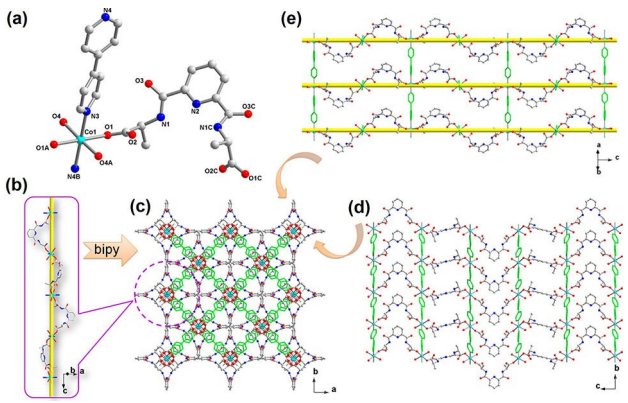

Figure 8. (a) Coordination environment of the Co(II) ion in $[Co(PDBAla)(bpy)(H_2O)_2].3H_2O$, (b) the single-stranded, right-handed [Co-PDBAla] helical chain running along the*c*-axis. The 3D framework of viewed from the (c) [001], (d) [100], and (e) [110] directions, respectively. Reproduced from Ref. 29 with the permission of the American Chemical Society.

variable counterions (BF_4^-, CMOM-2S; $CF_3SO_3^-$, CMOM-3S), or substitutions on organic linker (2-Cl, CMOM-11R; 3-Cl, CMOM-21R; 4-Cl, CMOM-31R; and 4-CH_3, CMOM-41R). The structural analysis of these crystalline sponges revealed that a combination of host-guest, guest-guest interactions and the pore adaptability play an important role in determining the enantioseparation abilities of these MOFs with hard-soft features enabling the chiral discrimination.[19a]

2.1.2 Chiral MOFs from Metallosalen Ligands

The metallosalens are another popular class of linkers used in the direct synthesis of the chiral MOFs. Constructed from salen ligands possessing the N_2O_2 binding pockets and metal ions (transition, main group and inner transition metals) that can adopt square planar, tetrahedral, square pyramidal and even octahedral geometries; these metallosalens are well-documented in the literature for a number of applications in asymmetric reactions, catalysis, sensing, molecular recognition and magnetic resonance imaging.[30] Due to their structural robustness, rich coordination chemistry, facile incorporation of chiral groups and asymmetric catalytic behavior, the metallosalens are an excellent functional strut to obtain chiral MOFs for a variety of applications.[31] A few examples of metallosalen ligands are shown in Scheme 3.

One such chiral pyridyl-substituted (salen)Mn complex: (*R*,*R*)-(−)-1,2-cyclohexanediamino-*N*,*N*′-bis(3-*tert*-butyl-5-(4-pyridyl)salicylidene)$Mn^{III}Cl$ (L^3) was used as a strut to generate the chiral MOF $[Zn_2(bpdc)_2L^3\cdot 10DMF\cdot 8H_2O]$ (bpdc: biphenyl-4,4′-dicarboxylic acid, DMF: dimethylformamide) by Cho and co-workers. The framework displayed an interpenetrating pair of networks with distorted rectangular and rhombic channels, whereby the ligands L^3 from the paired networks are parallel to each other and the Mn^{III} sites are easily accessible due to the diagonal displacement of the networks. Despite the presence of interpenetration, the MOF showed 57% solvent-accessible volume and could be used as a highly efficient catalyst for enantioselective epoxidation.[32]

Xia et al. developed the multivariate MOFs (MTV-MOFs) containing one, two or three different chiral metallosalen linkers in a single framework. Firstly, the salen linker N,N′-bis(3-tert-butyl-5-(carboxyl)salicylide (H_4L^4) was used to generate the dicarboxylate metallosalen ligands H_2L^{4M} [M: Cu, VO, CrCl, MnCl, Fe(OAc), and Co(OAc)] by reacting with the corresponding metal salts. The two-fold interpenetrated 1^{Cu}, $[Zn_4O(L^{4Cu})_3]\cdot 5MeOH\cdot 2DMF$ (MeOH: methanol) with primitive cubic (**pcu**) topology was then obtained by heating $Zn(NO_3)_2\cdot 6H_2O$ with H_2L^{4Cu} in DMF at 80 °C. The family of the multivariate MOFs with $Zn(NO_3)_2\cdot 6H_2O$ was then obtained by varying the ratios of different ligands: five binary MTV-MOFs (1^{CuV}, 1^{CuMn}, 1^{CuCr}, 1^{CuFe}, and 1^{CuCo}) from H_2L^{4M} [M: VO, CrCl, MnCl, Fe(OAc), and Co(OAc)] and H_2L^{4Cu} in 1:1 ratio; and two ternary MTV-MOFs (1^{CuMnCr} and 1^{CuMnCo}) from a mixture of one or two identical H_2L^{4Cu}, H_2L^{4Mn}, and H_2L^{4M} [M: CrCl and Co(OAc)] in a 1 : 1 : 1 ratio (Figure 9). The MTV-MOFs further demonstrated excellent activities as recyclable heterogeneous asymmetric catalysts for relevant asymmetric sequential alkene epoxidation/epoxide ring opening reactions.[33]

Another noteworthy work was carried out by Li and co-workers to generate a new class of "porphyrin-salen based chiral MOFs" (ps-CMOFs) assimilating the metalloporphyrin and the chiral metallosalen struts in a single MOF. Since the bulky molecular sizes of the porphyrin and the metallosalens could generate large voids in the framework leading to instability, the (*R*,*R*)-*N*,*N*′-bis(3-*tert*-butyl-5-(4-pyridyl)-salicylidene)-1,2-diphenyldiamine nickel(II) (NiL^5) was chosen as the metallosalen to allow for the strong π–π stacking interactions and space-filling effects from the diphenyl groups. The $[Cd_2(NiL^5)(CdL^6)][Cd_2(NiL^5)(H_2L^6)]\cdot 6DMF\cdot 5MeOH$ was

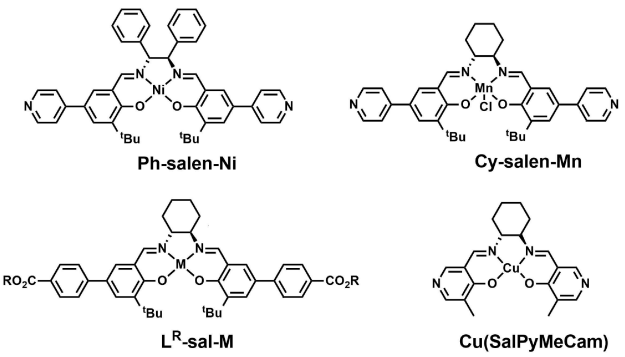

Scheme 3. Representative examples of metallosalen-based ligands.

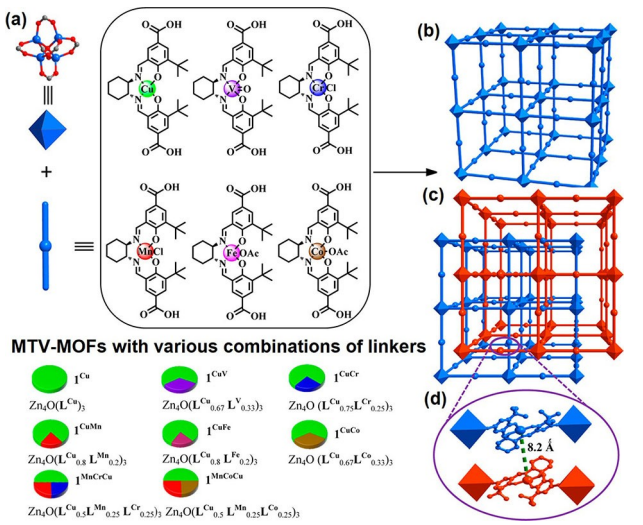

Figure 9. (a) Construction of MOF 1^{Cu} and corresponding MTV-MOFs 1^{CuM} and $1^{CuMM'}$ with different metallosalen linkers, (b) one 3D unit of MOF 1^{CuM}, (c) two-fold interpenetrating 1^{Cu} (red indicates the interpenetrated 3D network), and (d) close-up view of two L^{4Cu} units brought into proximity to each other by 2-fold interpenetration. Reproduced from Ref. 33 with the permission of the American Chemical Society.

obtained from tetra-(4-carboxyphenyl)porphyrin (H_6L^6), NiL^5 and $Cd(NO_3)_2 \cdot 6H_2O$ featuring two different types of interpenetrated networks ; one with a Cd(II) bound to the porphyrin core, and the other with metal-free porphyrin (Figure 10).

Here too, despite the interpenetration the framework has 1D channels with a solvent accessible volume of 52% and furthermore the MOF served as a highly effective catalyst in the asymmetric cyanosilylation of aldehydes. The authors attributed the excellent performance to the synergistic effect of the chiral induction from the metallosalen and the Lewis acidity of the metalloporphyrin.[34]

2.2 Indirect Methods

2.2.1 Post Synthetic Modification (PSM)

In this methodology, the chirality can be introduced on the achiral MOFs by post-synthetic modification of the active sites with chiral moieties through grafting, linker exchange or cation exchange. The PSM provides an approach to effectively generate MOFs bearing a variety of chiral functionalities which might be otherwise inaccessible, or tedious and relatively expensive to synthesize via conventional direct methods. The chiral functionalities can be introduced on both the organic linker struts as well as the metal clusters. Furthermore, new chiral MOFs can also be generated from the existing chiral ones using PSM.[17a–c,30b]

Based on this strategy, Bonnefoy and co-workers utilized three MOFs bearing -NH_2 groups with different topology, dimensionality and pore size: Al-MIL-101-NH_2, Zr-UiO-66-NH_2 and In–MIL-68-NH_2, (MIL: Matérial Institut Lavoisier) as the starting platforms to graft amino acids and peptides onto the frameworks. The pendant amine groups on the organic linkers provide the reactive centers to graft the chiral sites via covalent bonding. The post-functionalized MOFs were obtained by reacting an amino acid and various oligopeptides under microwave irradiations to obtain the grafted chiral solids. The Al-MIL-101-NH_2 having a large pore aperture was able to show the highest grafting yield; whereas the Zr-UiO-66-NH_2 showed negligible grafting yield towards various peptides owing to its small pore size.[35]

Zhuo et al. explored the solvent-assisted linker exchange (SALE) of ZIF-78 (ZIF: zeolite imidazolate framework) to prepare a pair of chiral S(R)-ZIF-78 h (Figure 11) with gmelinite (**gme**) topology, by replacing the 5-nitrobenzimidazole (5-nbim) with enantiopure (S or R)-2-(1-Hydroxyethyl) benzimidazole, (S(R)-OH-bim). The resultant homochiral S-ZIF-78 h exhibited high permanent porosity and was used for enantioselective sensing and separation towards D/L-proline.[36]

Chen and co-workers incorporated chiral salen(Co(III)) within the cages of a MOF through adsorption followed by PSM to generate the chiral MOF (*R*,*R*)-salen (Co(III))@IRMOF-3-AM (IRMOF: isoreticular MOF). The salen was first adsorbed into the pores of the MOF and then the free amine groups of IRMOF-3 were acylated using anhydride by PSM (Figure 12). This led to the acylamide groups acting as a fence to block the leaching of the salen complex from the window, thereby eliminating the need to modify the chiral active species and providing a strategy to

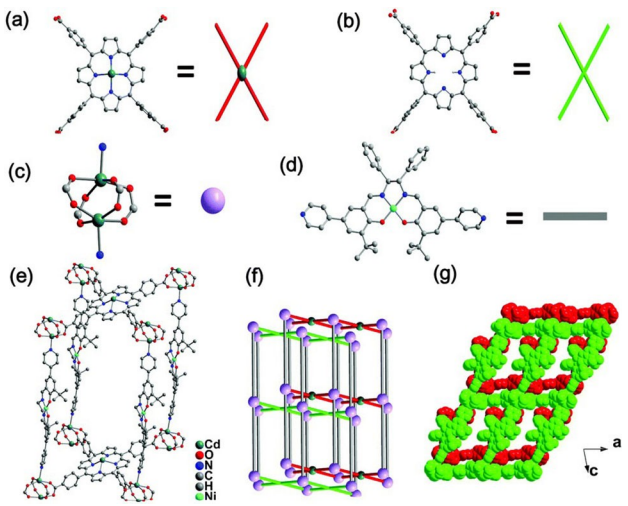

Figure 10. View of (a) CdL^6, (b) H_2L^6, (c) Cd-paddlewheel SBU, (d) NiL^5, (e) $[Cd_2(NiL^5)(CdL^6)][Cd_2(NiL^5)(H_2L^6)] \cdot 6DMF \cdot 5MeOH$, (f) topological structure of the 3D network of the MOF, and (g) space-filling view of the 2-fold interpenetrated network along the *b* axis. Reproduced from Ref. 34 with the permission of the Royal Society of Chemistry.

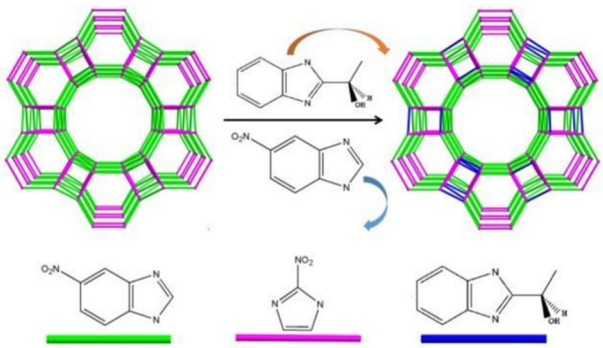

Figure 11. The synthetic strategy of ZIF-78 h. Reproduced from Ref. 36 with the permission of the Royal Society of Chemistry.

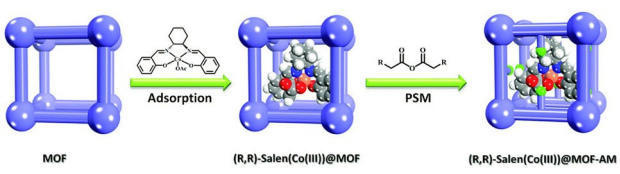

Figure 12. Schematic description of imprisoning of homogeneous chiral salen(Co(III)) catalyst within the cage of MOF in two steps. Reproduced from Ref. 37 with the permission of the Royal Society of Chemistry.

generate chiral MOFs whilst retaining the pristine form of the chiral moiety. Moreover, small reactants could still diffuse through the pores and were able to access the chiral active sites, thereby rendering this MOF as an efficient catalyst in the asymmetric catalysis for coupling CO_2 with epoxides.[37]

Although the PSM provides for a large scale and low-cost construction MOFs, however the modification efficiency or the extent of chiralization of the framework depends on several factors such as pore size, reaction conditions, efficiency of the reaction etc. Moreover, the parent framework should be chemically stable and able to retain its structural integrity after the PSM. Despite these challenges, its high feasibility and flexibility make it a widely used strategy to construct chiral MOFs.

2.2.2 Superficial Chiral Etching Process (SCEP)

The PSM leads to a decrease in the porosity of the framework and reduction in the pore size. A chiral modification on the outer surface would be optimal as it could provide chirality to the MOF without disturbing its inherent porosity.

Hou and co-workers utilized the superficial chiral etching process (SCEP) for designing hybrid (chiral-achiral) MOF having achiral core-structure MOF (Figure 13). Herein, the surface of achiral MOF $[Cu_3(btc)_2]$ (btc: 1,3,5-benzenetricarboxylate), behaved as a source of Cu(II) which reacts with (+)-Cam and 1,4-diazabicyclo[2.2.2]octane (dabco) paito generate $[Cu_2((+)\text{-Cam})_2dabco]$ (homochiral MOF) on surface of achiral MOF, which in turn led to the formation of $[Cu_3(btc)_2]@[Cu_2((+)\text{-Cam})_2dabco]$.The SCEP technique proved out to be the economically beneficial and one of the efficient methodology of selective enantioseparation of (S)-limonene against (R)-limonene.[38]

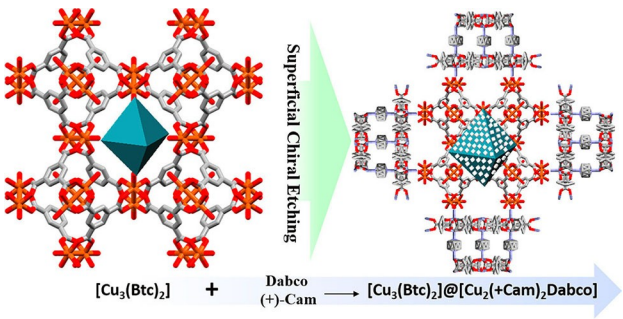

Figure 13. Schematic illustration of the superficial chiral etching process. Superficial layers of a presynthesized MOF of $[Cu_3(btc)_2]$ provides a Cu(II) source to react with (+)-cam and dabco, producing $[Cu_2((+)\text{-cam})_2dabco]$ on the surface of the achiral parent MOF, leading to an achiral MOF@homochiral MOF core–shell hybrid structure. Reproduced from Ref. 38 with the permission of the American Chemical Society.

2.2.3 Inducing Chirality into MOF

Herein, the chirality is induced into the framework by using the appropriate chiral templates such as solvents, chiral co-ligands as external additives or circularly polarized light. This method allows a cost-effective approach without the need for specialized linkers. Moreover, the properties of the generated chiral MOFs can be tuned easily through the design of the initial MOF.[30b]

Morris et al. demonstrated the induction of homochirality in a MOF built from achiral building blocks by through the chiral ionic liquid solvent 1-butyl-3-methylimidazolium L-aspartate (BMIm-L-asp). The resultant SIMOF-1 $(BMIm)_2[Ni(TMA\text{-}H)_2(H_2O)_2]$ (BMIm: 1-butyl-3-methylimidazolium, TMA: trimesic acid) featured bulk homochirality which was further proven by single crystal X-ray determinations of 10 different random crystals. Moreover, the ionic liquid BMIm without the chiral L-asp component generated achiral SIMOF-2, and the replacement of L-asp with D-asp generated SIMOF-1a with opposite chirality; thereby establishing the role of chiral ionic liquid guest to induce chirality in the MOFs.[39]

CMOF-5 (CMOF: chiral MOF), the chiral variant of the benchmark MOF-5 material was also obtained using the chiral induction method by Zaworotko and co-workers in 2015. The Λ-CMOF-5 and △-CMOF-5 were prepared by using the L-proline or D-proline, $Zn(NO_3)_2\cdot 6H_2O$ and H_2bdc in a 1 : 1 : 1 ratio with N-methyl-2-pyrrolidone (NMP) and water as the solvent system (Figure 14). The CMOFs crystallized in the chiral cubic space group $P2_13$ and the origin of chirality was

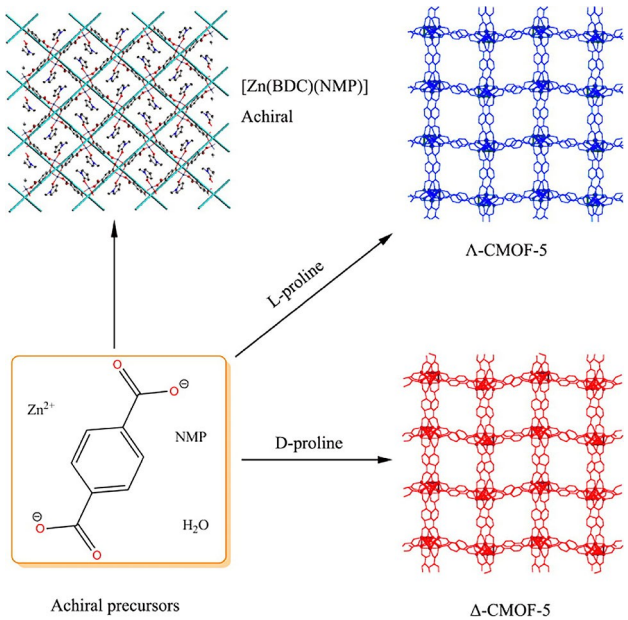

Figure 14. Synthesis of CMOF-5. The presence of L- or D-proline additives induces chirality and enables the growth and isolation of CMOF-5 crystals. An achiral square grid net, [Zn(bdc)(NMP)], forms in the absence of proline. Reproduced from Ref. 40 with the permission of the American Chemical Society.

attributed to the distortion in the backbone of the network with the atropisomer-like bridging mode shown by the linkers that translates chirality from one cluster to another. Achiral layered [Zn(bdc)(NMP)] was afforded in the absence of L-proline or D-proline, establishing the role of proline in the crystallization of Λ-CMOF-5 or △-CMOF-5.[40]

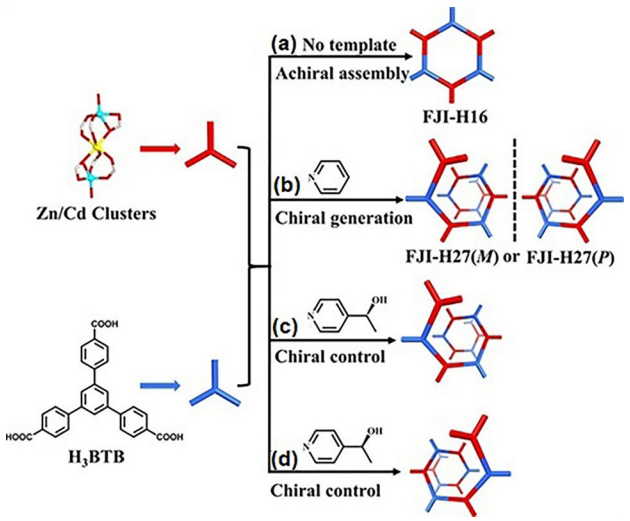

Figure 15. Chiral induction from achiral precursors through template-driven self-assembly process: (a) achiral self-assembly without template, (b) pyridine driven generation of chirality, (c) and (d) controlling chiral orientation and distribution of bulk FJI-H27 samples through targeted modification on pyridine. Reproduced from Ref. 41 with the permission of John Wiley and Sons.

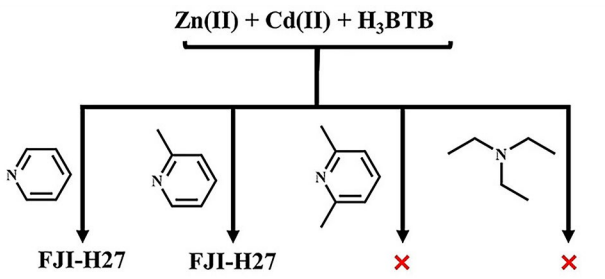

Templates / Chiral induction	(mmol)	(mmol)
Start induction	0.19	0.4
Partial induction	0.19 – 0.37	0.4 – 1.2
Complete induction	> 0.37	> 1.2

Figure 16. Chiral generation effect of different molecules. Reproduced from Ref. 41 with the permission of John Wiley and Sons.

More recently, Wu and co-workers reported the use of achiral external stimuli to generate chirality from achiral precursors, whereby a control in the chiral induction from no induction to partial and complete induction could be realized by a change in the reaction conditions. The FJI–H16 (FJI: Fujian Institute of Research on the Structure of Matter, Figure 15) constructed from benzene-1,3,5-tris(4-benzoic acid) (H_3BTB) and Zn(II)/Cd(II) clusters could be converted to the chiral 3D FJI–H27 (*M*) or FJI–H27(*P*) by controlling the amount of pyridine and the temperature (Figure 16). The pyridine molecules served as the template for chiral generation and the formation of chiral FJI–H27 was established to be a kinetically controlled self-assembly process. An intermediate FJI–H28 could be isolated from the chiral generation transition state, providing insights into the chiral generation mechanism of FJI–H27.[41]

2.2.4 Resolution

In this methodology, the chiral MOFs are developed from achiral fragments through crystallization in an enantiomorphous space group due to the simultaneous spatial organization of the building blocks. The crystallization breaks its symmetry and leads to formation of the chiral MOFs. However, in such a resolution process both enantiomers of the MOF are present, leading to a bulk racemic mixture. To achieve their practical utilities, the separation of the chiral MOFs is an essential step. Several homochiral MOFs have been identified by the self-resolution process providing significant crystal engineering information. Further investigations on the mechanistic aspects of the self-resolution process will be helpful to provide a deeper understanding and establish a generalization of this methodology.[17c,30b]

In 1999, Aoyama et al. showed the first example of a homochiral MOF obtained via self-resolution. Here, the MOF [Cd(L^7)(NO_3)$_2$(H_2O)EtOH] (EtOH: ethanol) was built from Cd(NO_3)$_2$·4H_2O and 5-(9-anthracenyl)pyrimidine(L^7); and the chirality arose due to the pyridine-Cd(II) helical array which could be controlled chiral seeding during the crystallization as well as through solid-state helix winding.[42]

In the case of an achiral ligand bearing inherent conformational chirality, self-resolution can be achieved by locking the specific chiral conformation via coordination (Figure 17). Cui and co-workers utilized tetrakis(4-(pyridin-4-yl)phenyl) ethylene (TPPE), a pyridyl functionalized tetraphenylethylene ligand for the spontaneous resolution of the [Co(TPPE)Cl_2]·4DMF whereby both the enantiomorphic forms M and P were unambiguously probed by single crystal X-ray diffraction measurements. Furthermore, the chiral MOF could act as a crystalline sponge for the adsorption and structural determination of six guests, of which the 2-butanol and 2-butylamine were enantiospecifically crystallized.[43]

More recently, Lahav, van der Boom and coworkers reported a fascinating new aspect of obtaning chirality at the molecular and morphological levels from achiral

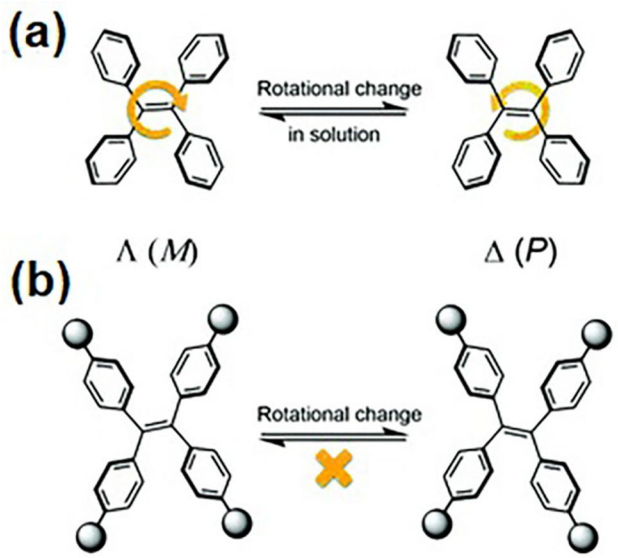

Figure 17. (a) The free rotation of the TPE core in solution, and (b) the rotation inhibition through coordination-induced fixation. Reproduced from Ref. 43 with the permission of the Royal Society of Chemistry.

components.[44a–b] Metallo-organic single crystals with a multi-domain morphology were obtained from the morphologically achiral seeds posessing homochiral channels and the rare space group *P*622. The framework was constructed from Cu-$(NO_3)_2 \cdot 3H_2O$ and the achiral linker 1,3,5,7-tetrakis(4-(pyridyl-4'-yl-ethynyl)phenyl)adamantine (TPEPA) generating the "yo-yo" like structures with opposite helicity (Figure 18). The authors attributed the presence of the chiral packing arrangement to the propeller-type coordination arrangement of the pyridine units connected to the central Cu(II).[44c]

Another example of the individually chiral surface bound and oriented MOFs (sMOFs) was reported by the same group whereby chirality at different levels is also achieved from the crystallographic packing. Modulation of the counteranions, metal cations and growth environments led to nearly identical chiral frameworks. A macroscopic oriented growth of metallo-organic crystals using 1,3,5,7-tetrakis(4-((E)-2-(pyridin-4-yl)-vinyl)phenyl)adamantane (Ad-DB) with NiX2 (X = Cl^-,Br^-, $NO3^-$, or CH_3COO^-) was achieved with a control over the crystal dimensions and morphology.[44e] Other morphological variants of chiral and single crystals were also obtained,[44d,f] opening completely new avenues for achieving chirality at molecules and macromolecular level from achiral precursors.

3. Enantioselective Separations Using Chiral MOFs

The most significant application of chiral MOFs is in the enantioselective separation of chiral molecules owing to their

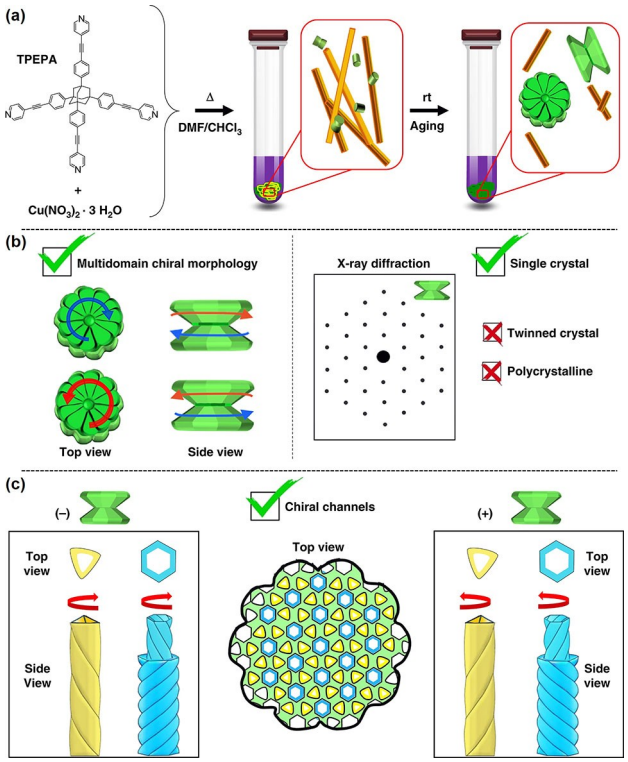

Figure 18. (a) solvothermal reaction of the achiral organic ligand TPEPA with copper(II) nitrate, followed by aging of the sample at room temperature, (b) the single crystals display chiral features at morphological levels: an off-set angle between the constituting disks and a spiral growth phase (left) and X-ray diffraction studies reveal the single crystallinity of the entire, morphological complex structure (right), and (c) the crystal structure consisting of continuous helicoidal channels. Each crystal is enantiopure whereas the bulk sample is racemic. Reproduced from Ref. 44c with the permission of Springer Nature.

ultrahigh porosity, highly specific chiral recognition sites and pore size tunability to assist in separation of the isomers. The chiral MOFs are being extensively utilized for separation of a variety of enantiomers such as drugs, amino acids, biomolecules and chiral organic molecules (alcohols, hydrocarbons etc.). Moreover, these chiral MOF adsorbents have demonstrated cost-effective and highly efficient rapid separation of the enantiomers. In this section, we discuss the illustrative examples of the separation of various classes of enantiomeric racemates.

3.1 Separation of Chiral Alcohols

In 2012, Das and co-workers synthesized a series of M-MOFs: $Cd_3(bdc)_3[Cu(SalPyMeCam)] \cdot (G)_x$, $Cd_3(bdc)_3[Cu(SalPytBuCy)] \cdot (G)_x$, $Zn_3(cdc)_3[Cu(SalPyMeCam)] \cdot (G)_x$ and $Zn_3(cdc)_3[Cu(SalPytBuCy)] \cdot (G)_x$ (cdc: 1,4-cyclohexanedicarboxylate) by employing metallo- as well as organic ligands. These M–MOFs were found to have the potential to separate

chiral alcohols viz. BUT (2-butanol), 2-PEN (2-pentanol) and PEA (1-phenylethanol). The M-MOF $Zn_3(cdc)_3[Cu(SalPytBuCy)]\cdot(G)_x$ was found out to be highly efficient for separating 1-phenylethanol with maximum ee of 82.4%.[45]

A pyridyl functionalized metallosalan 6,6′-((((1R,2R)-cyclohexane-1,2-diyl)bis(azanediyl))bis(methylene))bis(4-(tert-butyl)-2-((E)-2-(pyridin-4-yl)vinyl)phenol) (H_2L^8) was reacted with $ZnCl_2$ for construction of helical and chiral MOFs: (R)-$[Zn_8L^8{}_4Cl_8]$ and (R)-$[Zn_8L^8{}_4Cl_8]\cdot THF\cdot H_2O$ (THF: tetrahydrofuran) having chiral octa-nuclear cages. The cavities exhibited fluorescence enhancement in the presence of amino acids such as alanine, phenylalanine and valine; but the maximum enhancement was observed in the presence of alanine with (R)-$[Zn_8L^8{}_4Cl_8]\cdot THF\cdot H_2O$, attributed to the bulky phenyl groups. The MOFs were then explored for their selective separation of four alcohols such as 1-phenylethylamine, 1-phenylpropanol, 1-(methylsulfinyl) benzene and 1-phenylethanol and the enantiomeric excess was calculated to be 14.6%, 13%, 20% and 4.7% respectively. It was inferred that (R)-$[Zn_8L^8{}_4Cl_8]\cdot THF\cdot H_2O$ gave maximum fluorescence enhancement in the presence of (S)-1-(methylsulfinyl)benzene with ee of 37.5%, (S)-1-phenylpropanol with ee of 18.6%, (S) phenylethanol with ee of 13.8% whereas, the enantioselectivity for (S)-phenylethylamine was found out to be less, with ee of 10.3%.[46]

Zhang et al. synthesized $[Co_2(IN)_4(H_2O)]_n$ (IN: isonicotinic acid) from achiral precursors which included both the enantiomers : right and left. The enantioselective mechanistic pathway was proposed through hydrogen bonding as depicted by single-crystal-to-single-crystal process. When the enantioselectivity was explored, both the enantiomers were selective towards 1-phenylethanol, through hydrogen bond to form $[Co_2(IN)_4(H_2O)]_n$(right)⊂(R)-1-phenylethanol and $[Co_2(IN)_4(H_2O)]_n$(left)⊂(S)-1-phenylethanol. This report was claimed to be the first example wherein, homochiral MOFs were used for chiral recognition of 1-phenylethanol.[47]

A pair of 2D CCPs (chiral coordination polymers) viz. $[[Cd(L\text{-}cps)_4\cdot(bix)_4]\cdot(CH_2Cl_2)_2(EtOH)(H_2O)]_n$ and $[[Cd(D\text{-}cps)_4\cdot(bix)_4]\cdot(CH_2Cl_2)_2(EtOH)(H_2O)]_n$ were prepared by Lu et al. for the selective sorption of 1-phenylethanol. The polymers were built via self-assembled chiral metal-camphor-10-sulfonate (cps) salts $[Cd(L\text{-}cps)_2\cdot(H_2O)_6]$ and $[Cd(D\text{-}cps)_2\cdot(H_2O)_6]$ and bidentate ligand (bix: 1,4-bis(imidazole-1-yl-methyl)benzene) which decides the inclusion of S and R-PEA having enantioselectivity ratio of 9 : 1. The enantioseparation was achieved with the enantiomeric excess (ee) value of 28.2% for separation of R-PEA by L-enantiomer whereas, D-enantiomer could separate S-PEA with ee value of 27.3%.[48]

In general, the efficiency of separation of isomers is directly proportional to the number of functional groups available for interaction with sorbent. Satska and co-workers developed chiral PCPs $[Zn_2(bdc)(Lact)(DMF)]_n\cdot nDMF$, $[Ni_2(asp)_2(bpy)]_n\cdot nCH_3OH\cdot nH_2O$ and $[Co_3(TMTA)_2(bpy)_4]_n\cdot 28nH_2O$ ($Lact^{2-}$: (S)-lactate, TMTA: trimesoyl-(S)-alanine) for studying the selective sorption of optically pure isomers of 2-butanol (from gas phase). PCPs $[Zn_2(bdc)(Lact)(DMF)]_n\cdot nDMF$, $[Ni_2(asp)_2(bpy)]_n\cdot nCH_3OH\cdot nH_2O$ were capable of selective sorption of R-2-butanol, whereas the PCP $[Co_3(TMTA)_2(bpy)_4]_n\cdot 28nH_2O$ gave better sorption for S-2-butanol.[49]

Zhang et al. reported the formulation of two enantiomorphic homochiral MOFs $[Cd[(S)\text{-}PIA](Hdabco)]_n$ and $[Cd[(R)\text{-}PIA](Hdabco)]_n$, (PIA: (R)-5-(2-carboxypyrrolidine-1-carbonyl)isophthalic acid) which were built from proline-based ligands. Both the HMOFs showed features which included presence of four helical chains and three different types of helical channels. The size of the helical channels was appropriate for selectively adsorbing methyl lactate with high ee of 65.8% for (S)-isomer and 68.3% for (R)-isomer whereas, the ee values for (R) and (S) isomers of ethyl lactate and 1-phenylethanol were 12.1%, 14.9% and 5.3% and 5.6% respectively.[50]

Enantiopure (1S)-1-(5-tetrazolyl)-ethylamine (5-eatz) was used to construct homochiral porous MOF $[[Cu^1{}_2u^{11}(5\text{-}eatz)(CN^-)(H_2O)]^+[NO^-{}_3]]\cdot[DMF]$ having unusual ligand-unsupported Cu–Cu interactions which contributes to its stability in water and other organic solvents. On examining the enantioselectivity towards different aliphatic and aromatic alcohols, the results revealed that the homochiral MOF could resolute the racemates of aromatic alcohols, (R,S)-1-phenylethanol and (R,S)-1-phenylpropanol with 42% ee (R) and 48% ee (R); whereas the enantioselectivity for aliphatic alcohols such as 2-butanol and 2-methyl-2,4-pentadiol was less than 5% ee.[51]

Chiral 3D network MOF $[Co_2(H_2O)(cpda)_2(py)_4py]_n$ (H_2cpda: trans-(S,S)-1,2-cyclopropane dicarboxylic acid, py: pyridine) was obtained and the structure was elucidated by single-crystal XRD. Chiral centers in ligand are constructed form 3 non-polar fragments and one polar carboxyl group. The coordination polymer was formed by joining Co(II) with trans S,S cyclopropane dicarboxylate wherein, the $cpda^{2-}$ ions were used to link three Co(II) ions, two of those were linked via 1 carboxylate ion whereas, the other carboxylate of $cpda^{2-}$ was bound via one oxygen atom, to one Co(II). To compare the sorption of the prepared Co(II)-MOF, two previously reported Zn-complexes: $[Zn_2(cam)_2(bpy)\cdot 3DMF\cdot 2H_2O]_n$ and $[Zn_2(cam)_2(dpe)\cdot 5DMF\cdot H_2O]_n$ (dpe: trans-1,2-di(4-pyridyl) ethylene) were chosen. For examining their enantioseparation of racemic mixture of 2-butanol, the desolvated complexes were prepared. It was observed that $[Co_2(H_2O)(cpda)_2(py)_4]$ (desolvated complex) preferred sorption for S-butanol, the Zn complexes $[Zn_2(cam)_2(bpy)\cdot 3DMF\cdot 2H_2O]_n$ (desolvated complex) for S-butanol, and the $[Zn_2(cam)_2(dpe)\cdot 5DMF\cdot H_2O]_n$ (desolvated complex) towards R-butanol.[52]

Kolotilov and co-workers formulated Zn-based and Na-based homochiral coordination polymers having formulas $[Zn_2(bdc)(S\text{-}Lact)(DMF)]n$ and $Na_7[(VO)_7(H_2O)_7(\beta\text{-}CD)_2]$ (CD: cyclodextrin), respectively wherein the chirality is induced in the homochiral PCPs by S-Lactate and β-CD units. The Zn-based PCP was capable of effectively separating 1-phenylethanol whereas, Na-based PCP resoluted the 2-butanol

having ee of 5.4%±1.5% for (S)-enantiomer which may be attributed to the adsorption capacity of the Na-based PCP.[53]

Two enantiopure chiral PCPs were prepared by using L/D-alanine and $Zn(CH_3COO)_2 \cdot 2H_2O$. It was further subjected to enantioseparation of 1-phenyl-1-propanol, which is an important scaffold for preparation of different chiral drugs e.g. salbutamol. The enantiomeric excess of 1-phenyl-1-propanol as determined by the D-isomer PCPs was maximum (42.86%) at lower concentration of alcohol, but it decreased (34.78%) with further increase in concentration of the alcohol. In addition to this, when the D-PCP was suspended in racemic alcohol directly, similar results were attained. But, when the temperature was increased (25 °C), the ee value also increased to 44.58%.[54]

Chiral Cd based 3D MOF was developed by Cui et al., from an enantiopure carboxylate ligand of 1,1′-biphenol: ((S)-3,3'-dibromo-6,6′-dimethyl-5,5′-di(3,5–bis(methoxy carbonyl) phenyl-1,1′-biphenyl-2,2-diol). The Cd–MOF was able to successfully separate 1-(4-fluorophenyl) ethanol, 1-(4-chlorophenyl) ethanol, and 1(4-bromophenyl) ethanol, with 93%, 98%, and 98% ee values, respectively. Apart from alcohols, different sulfoxides could also be separated such as methyl phenyl sulfoxide, ethyl phenyl sulfoxide, 3-methoxyphenyl methyl sulfoxide, and 4-methoxyphenyl methyl sulfoxide. The enantioselectivity range as revealed by the data was from 80 to 96%.[55]

A new strategy was followed by Das and co-workers for deriving chirality enriched MOF from racemic mixture of MOFs. Herein, the MOF [Eu(BTC)(H_2O)·DMF] with (+)/(−)-2-amino-1-butanol as chiral dopant (P/M ; plus & minus) was developed (Figure 19). It was further used to carry out the separation of chiral amino alcohols, (+/−)2-amino-1-butanol, (+/−)1-amino-2-propanol, (+/−)2-amino3-methyl-1-butanol, (+/-)2-methyl-2,4-pentanediol.[56]

Formation of CD-MOF which acted as a chiral selector and polyethersulfone (PES) as a matrix was given by Wang and co-workers. The CD-MOF/PES MMM (MMM: mixed matrix membrane) with a 20 wt% CD-MOF loading achieves a stable and nearly 100% enantioselectivity of R-(+)-1-phenylethanol over S-(−)-1-phenylethanol when non-polar n-hexane is used as the solvent.[57]

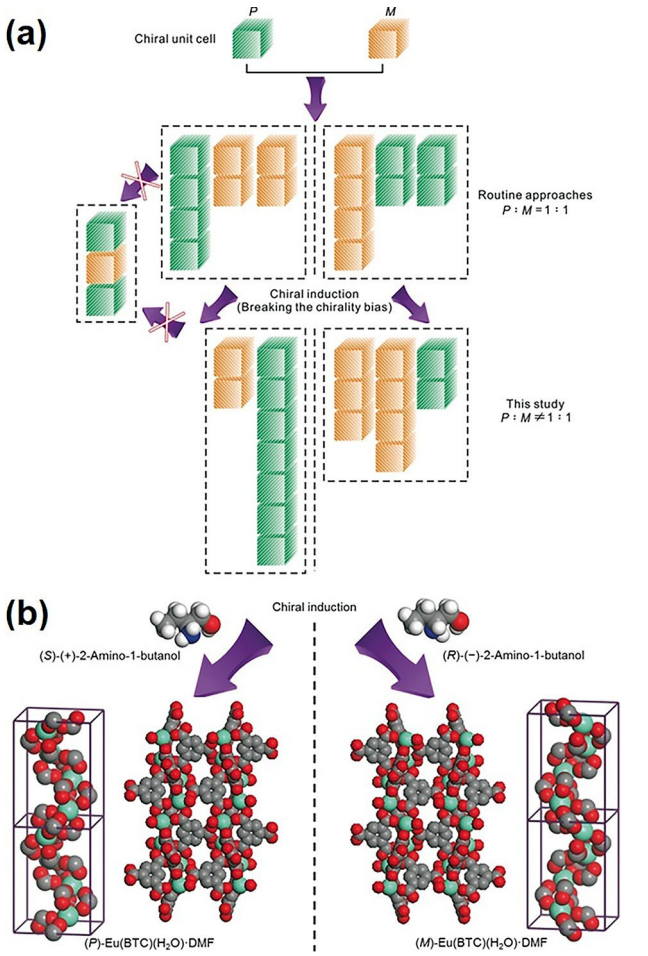

Figure 19. (a) Illustration of the strategy with reference to a chiral unit cell, and (b) incorporation of chiral dopants to afford the CE-MOFs (chirality-enriched MOFs). Reproduced from Ref. 56 with the permission of John Wiley and Sons.

3.2 Separation of Racemic Drugs, Biological Molecules and Amino Acids

It was in 2012, that the first chiral MOF was developed for selectively separating chiral drug racemates. Wang et al. synthesized and used a homochiral MOF [Zn_2(bdc)(L-lac)(DMF)](DMF) (L-lac: L-lactate) referred to as Zn-BLD by reacting metal ion (primarily Zn^{2+}), chiral fragment and the organic linker. Zn-BLD was capable of enantioseparating (S)-MPS (methyl phenyl sulfoxide) over R-MPS.[58]

Homochiral metal−organic zeolite (MOZ-51), having paracelsian (**pcl**) topology, was constructed by mixing D-camphoric acid and 5-methyl tetrazole ligands. It was used for chiral separation of racemic D/L-alanine methyl ester hydrochloride (through ion exchange process).[59]

Four homochiral 3D networks from combination of two organic tectons (with oxalate moieties) tect-1 (stereocenter C*HMeEt) having (R,R) enantiomer and tect-3 (stereocenter C*(CH2)MeEt) having (S,S) enantiomer with either Cu(II) or Zn(II) (in DMF), were developed by Sozzani and co-workers. Tect-1 or tect-3-Zn(II) were unstable in DCM and hence solvent-exchange couldn't be performed to form porous crystals whereas, both Cu- complexes were activated easily and was further examined for enantioseparation. It was observed that tect-3-Cu porous captures 66% and 20% L and D-tryptophan (after 30 min) whereas, Cu(II)-complex with tecton 1 could not be used.[60]

The evaluation of three chiral MOFs for enantioseparation of biologically active compounds in liquid phase was done by Calero and co-workers. The chiral MOF is composed of Cd atoms axially surrounded by (R)-6,6'-dichloro-2,2'-dihydroxy-1,1'-binaphthyl-4,4'-bipyridine linker connected to central

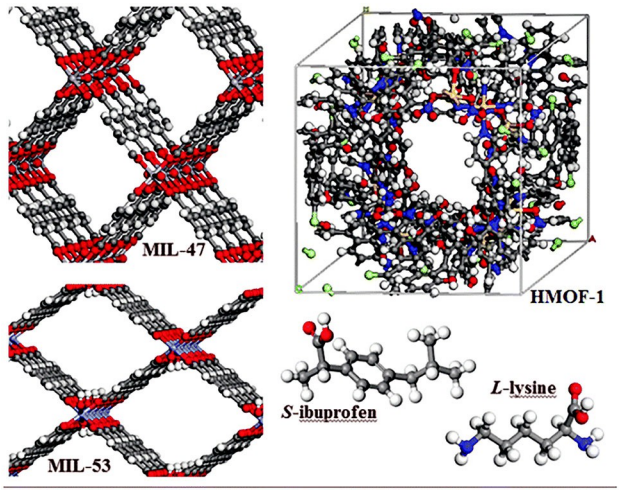

Figure 20. Front view of the unidirectional channels in MIL-47, MIL-53 and HMOF-1 along with the molecular representation of *S*-ibuprofen and L-lysine. Reproduced from Ref. 61 with the permission of the Royal Society of Chemistry.

metal and with the presence of helical pores (Figure 20). It was further applied for separation of racemic mixtures however, hetero-selectivity was observed for of ibuprofen's (an analgesic as well as anti-inflammatory drug) scalemic mixtures by using MIL-53 and MIL-47 (non-chiral) fragments. The lysine racemates were also resolved by the homochiral MOF-1 (HMOF-1).[61]

Feng and co-workers constructed a MOF with sodalite (**sod**) topology; D-His-ZIF-8 via LIS (ligand in situ) substitution of 2-methylimidazole with D-histidine. The MOF was further examined for its capability to resolute racemates and it was revealed that it could efficiently separate racemic alanine and glutamic acid with ee 78.52% and 79.44%. The enantiomers were then easily extracted with changing the properties of the MOF.[62]

It is also quite interesting to intermix chiral selector homochiral porous MOFs with graphene nanocomposites/sheets. Two MGO-based MOFs nanocomposites were prepared by Zhang et al. Firstly, Magnetic graphene oxide-metal (MGO) organic framework MGO-ZnBND: $[Zn_2(BTC)(NO_3)(DMA)_3]_n$ was developed which was efficiently employed for selectively capturing chiral drugs intermediates. The nanocomposite of the MGO-MOF reflected excellent properties of each and every component and also showed excellent enantioselectivity for 2,2'-furoin and benzoin with enantiomeric excess (ee) values up to 85% and 66%. Further, the host MGO-MOF was recycled by simply washing with methanol without any significant loss in the performance.[63]

3.3 Enantiomeric Separation of Chiral Hydrocarbons and other Organic Molecules

Bao and co-workers explored the Cd-BINOL MOF (BINOL: 1,1'-bi-2- naphthol) for separating the enantiomers of DMA ((R,S)-1,3-dimethylallene), DMP ((R,S)-dimethylcyclopropane and DMB ((R,S)-1,2-dimethylcyclobutane by following molecular simulation strategy. The DMA fragments were found out to easily fit into the pore size than the other chiral hydrocarbons, and hence achieved higher enantiomeric excess of 50%.[64]

A novel quantum dot (QD) based chiral MOF referred to as QD@MOF, was developed for the first time by Hou and co-workers, by combing enantioselectivity of the MOF, $[Zn_2(cam)_2(bpy)]$ and quenching of the CdTe quantum dots. The sensing method exhibited excellent results and was visual as well as convenient. The quantum-dot based MOF was further found out to be capable of enantioselectively and visually sensing of D- and L-tartaric acid.[65]

A number of zeolite type MOFs have been prepared earlier which were built from clusters of $[Cu_4I_4]$ and dabco. Similarily, homochiral zeolite-like MOF$[(Cu_4I_4)(dabco)_2]$. $[Cu_2(bbimb)]\cdot 3DMF$ (JLu-Liu23, JLu: Jilin University, H_2bbimb: 1,3-bis(2-benzimidazol)benzene) developed from achiral fragments, capable of hosting DNA (deoxyribonucleic acid) like double helical structure of $[Cu_2(bbimb)]_n$ polymers (Figure 21). This was claimed to be the first report on formulation of a unique homochiral and helical gyroid metal-organic framework attributed to the host-guest interactions.

Furthermore, JLU-Liu23M was prepared by inducing (−) cinchonidine or S-BINOL and JLU-Liu23P was prepared by the counter enantiomers of BINOL. As the MOF was prepared from achiral precursors and hence it was used for isolation of both enantiomers 23P and 23M. The JLU-Liu23M exhibited enantioselectivity towards methyl lactate with ee value upto 27%.[66]

4. Enantioseparation Using Chiral MOF Membranes and Thin-Films

Enantioselective membranes can be deployed for separating enantiomers from racemic mixture having different affinities. For chiral recognition either the chiral selector or the membrane material should have chiral sites. The membrane-based chiral separation has garnered immense interest due to its immense potential in the separation of chiral molecules at the preparative scale and it boasts of low cost, high capacity, trivial scale-up and continuous process.[17b]

Homochiral zeolitic imidazolate framework-8 (ZIF-8) membrane $[Zn(Hmim/L\text{-}His)_2]$: Hmim = 2-methylimideazolate and L-His = L-histidine, was synthesized by incorporating the natural amino acid L-His (Figure 22). The homochiral L-His-ZIF-8 membrane exhibited a good selectivity for the R-

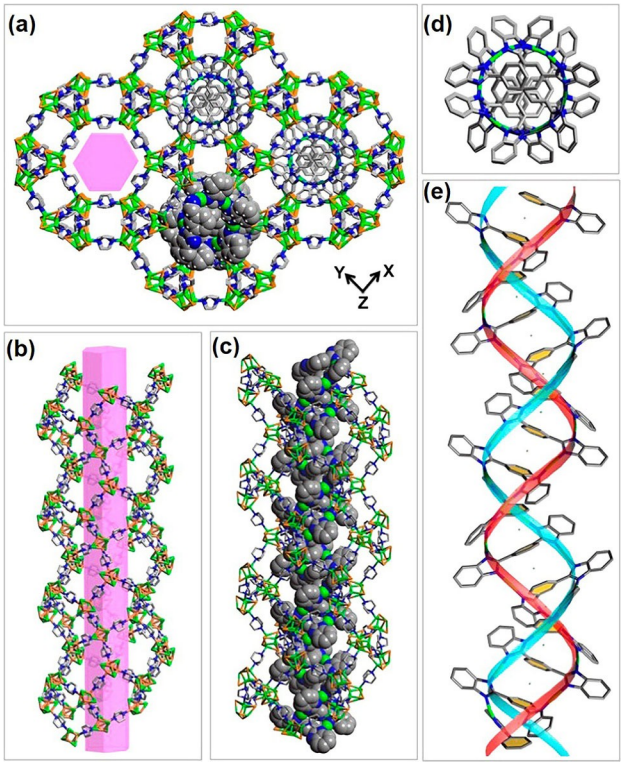

Figure 21. (a) The structure of JLU-Liu23 showing the interpenetrated 3D framework and double-helical chain, (b) helical channel formed by helical five-ring ribbons, (c) double-helical chain filled in the helical channel, (d) and (e) DNA-like double-helical chain viewed along the [001] and [110] directions, respectively. Reproduced from Ref. 66 with the permission of the American Chemical Society.

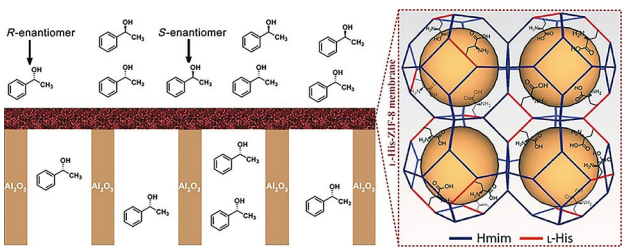

Figure 22. A representation of a homochiral L-His-ZIF-8-membrane for separating the *R*-enantiomer of 1-phenylethanol from the *S*-enantiomer. Reproduced from Ref. 67 with the permission of John Wiley and Sons.

enantiomer of 1-phenylethanol over the S-enantiomer, showing a high enantiomeric excess value up to 76%.[67]

The first homochiral MOF, efficient of carrying out the separation of diols was reported by Huang and co-workers in 2013. The MOF membranes were developed by opting secondary growth method, first step followed was generation of seed crystals via dip-coating method wherein, Al_2O_3 was seeded with MOF Ni-LAB $[Ni_2(L\text{-}asp)_2(bpy)]$ membrane seeds for 20s. The next phase was the secondary growth process, which involved the reaction of $NiCO_3$ and L-aspartic acid, in water at high temperature. Then 4,4'-bipyridine and methanol were added and seeded-support was autoclaved (keeping seeded side downwards) by placing into Teflon-lined stainless steel. The membrane was attained after heating the whole precursor was heated to high temperature. The MOF membrane was further studied for the potential to resolute racemic MPD (2-methyl-2,4-pentanediol), and could selectively separate R-MPD with maximum enantiomeric excess at low temperatures i.e. ~73.5% at 5 °C. Whereas, at 1 mmol L^{-1} feed concentration highest ee value of 35.5±2.5% (at 30 °C).[68]

Yan and co-workers developed a logic device as well as half-adders, based on the fluorescence changes during selective recognition of enantiomer. This involved the fabrication of enantioselective membranes [Eu@ZnCar@ZnO] wherein, ZnCar was prepared by reacting $Zn(NO_3)\cdot 6H_2O$ and carnosine (β-alanyl-L-histidine) in mixture of DMF and deionised H_2O. The membrane exhibits preferential sensing performance to R-penicillamine (R-Pen) over S-penicillamine (S-Pen) accompanied by a ratiometric luminescence response.[69]

Cui and co-workers for the first time developed a methodology wherein non-selective catalysts were converted to efficient enantioselective catalysts when introduced in nanostructured MOF. Two 3D porous and layered MOFs $[Zn_4(\mu_4\text{-}H_2O)(TBSC)][L^9]_2\cdot 3DMF\cdot CH_3OH\cdot 6H_2O$ and $[Zn_4(\mu_4\text{-}H_2O)(TBSC)][L^{10}]_2\cdot DMF\cdot CH_3CN\cdot 7H_2O$ (TBSC = p-tert-butylsulfonyl calix[4]arenes, L^9 = ligand prepared from (R) or (S) 2,2'-diethoxy-1,1'-binaphthalene and L^{10} = (R) or (S)-5,5',6,6'-tetramethyl-3,3'-dibromo-1,1'-biphenyl-2,2'-diol. Additionally, corresponding ultrathin MONs-2D (MON: metal-organic nanosheets) were also prepared. Both MOFs as well as MONs were also used as fluorescent sensors for distinguishing between chiral amino alcohols and the selectivity ratio were found out to be 1.4 and 2.3 times higher than of diols. Hence, chiral diol catalysts were boosted from being non-selective to enantioselective by installing them in nanostructured-MOFs.[70]

By modifying PSM methodology, Liu et al. followed PDM (post deposition chemical modification) to prepare multilayered h-SURMOFs (surface mounted MOFs). The distribution of functionality were controlled, and the layering involved hybrid binary surface-MOF having active and inert multilayers of $[Cu_2(NH_2\text{-}bdc)_2(dabco)]$ (active) on MOF $[Cu_2(bdc)_2(dabco)]$ (inert) and the ternary SURMOF $[Cu_2(ndc)_2(dabco)]$ (inert) over $[Cu(NH_2\text{-}bdc)_2(dabco)]$ (active) and $[Cu_2(ndc)_2(dabco)]$ (inert) (ndc: 2,6-naphthalene dicarboxylate). These multi-layers were prepared via LPE (liquid phase epitaxial) which makes it easy to fabricate these complex structures by introducing variety of pre-defined functionalities as well as pore size in the material. Presenting a future scope, it was believed to give excellent results for advanced enantioseparation i.e. they could be used as CSP for GC PLOT (porous layer open tubular) columns for separating complicated racemates.[71]

The effect of pore size on enantioselectivity of chiral isoreticular MOFs was explored by Heinke and co-workers. The isoreticular pillared and layered homochiral MOF [Cu_2(D-cam)$_2$(L^{11})] having chiral linkers (1R, 3S)-(+)-camphoric acid, connecting the layers and L^{11} are the pillar linkers which are generally the N containing donor ligands such as dabco, bpy and BpyB (1,4-di(pyridin-4-yl)benzene) (Figure 23). The enantioselective sorption of R- and S-limonene by MOF thin films having different N-linkers i.e. [Cu_2(D-cam)$_2$(dabco)], [Cu_2(D-cam)$_2$(BpyB)] and [Cu_2(D-cam)$_2$(bpy)] was investigated through QCM (quartz crystal microbalance). The ee values for resolving (S)-limonene vs. (R)-limonene by the MOF thin films were found out to be maximum for [Cu_2(D-cam)$_2$(bpy)] with 35% ee, 17% ee for [Cu_2(D-cam)$_2$(dabco)] and minimum for [Cu_2(D-cam)$_2$(BpyB)] with 8% ee. Similar experiments were conducted by employing SURMOFs having medium pore size, and enantiomeric excess for (R) vs. (S)-limonene was calculated to be 34% which is comparable with the ee determined for [Cu_2(D-cam)$_2$(bpy)] by QCM.[72]

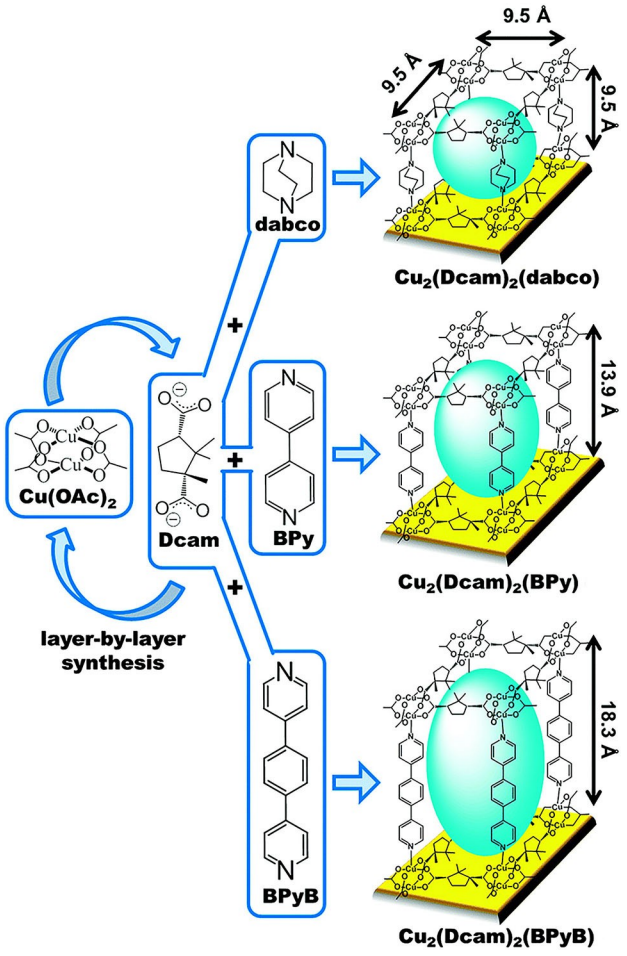

Figure 23. Isoreticular homochiral SURMOFs of type [Cu_2(D-cam)$_2$(L^{11})] with tunable pore sizes (L^{11}: dabco, Bpy or BpyB) prepared in a layer-by-layer fashion. Reproduced from Ref. 72 with the permission of the Royal Society of Chemistry.

Layered multicomponent MOFs (general formula: [$M_2L^{12}{}_2P]_n$, L^{12}: any carboxylate linker, and P: dinitrogen pillar ligand) are considered to be most favorable for LPE (M: Zn^{2+}, Cu^{2+}) and hence, SURMOF (+)/(-)[[Zn_2(cam)$_2$(dabco)]$_n$] was prepared by Fischer and co-workers. The synthesized SURMOFs were further examined for studying the adsorption of (R/S)-2,5 hexandiol (HDO) with enantiomeric excess of 64% (of R-HDO by (+)-SURMOF) and 66% (of S-HDO by (−)-SURMOF).[73]

Wattanakit and co-workers prepared chiral zeolite-imidazolate based framework: ZIF-8 from zinc(II) and 2-methyl imidazole. The electrochemical deposition/ dissolution strategy was adopted for electrodeposition of the metal via colloidal crystal template and then electro-oxidation was done, leading to generation of metal ions which interacted with chiral network to for MOFs. This zeolitic framework was used as a stationary phase in a microfluidic electrochromatographic device (Figure 24) for enantioselective adsorption and separation of D/L-tryptophan. The potential difference between chiral analyte and stationary phase gave a baseline separation of the enantiomers.[74]

Homochiral MOF grown on hydroxyl and carboxyl substrates gave homochiral porous MOF thin films (SURMOF) [Cu_2(D-cam)$_2L^{13}]_n$ (L^{13} = dabco or bpy). When hydroxy group with MUD (11-mercaptoundecanol**)** and carboxyl group with MHDA (16-mercaptohexadecanoic acid) were selected, the chiral-SURMOF showed its preferential growth along [001] and [110] orientation. The enantioselectivity and adsorption rates of D/L- isomers of methyl-lactate in [001] and [110] direction were studied by gas phase quartz crystal microbalance.[75]

Homochiral Surface-mounted MOF (SURMOF) film [Cu_2(D-cam)$_2$] having linkers dabco or bpy, were developed by layer-by-layer LPE process using selectively functionalized (-OH or poly(L-dopa) (dopa: 3,4-dihydroxyphenylalanine) substrates which results in the formation of MOF thin films. The enantioseparation was carried out by growing the thin film of MOF and MOF grown on poly(L–dopa) on capillary column of GC through LPE method. The obtained capillary

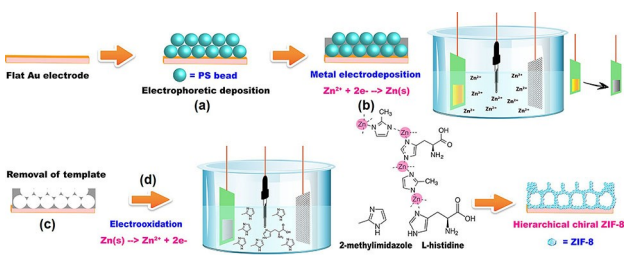

Figure 24. Illustration of the synthesis steps of hierarchical macroporous chiral ZIF-8, including (a) PS (phosphatidylserine) bead assembly via electrophoretic deposition, (b) electrodeposition of macroporous zinc, (c) removal of PS beads, and (d) electrodissolution of zinc in the presence of organic ligands. Reproduced from Ref. 74 with the permission of the American Chemical Society.

column was then used for resolution of methyl lactate (with dabco linker) and phenylethanol (with bpy linker).[76]

The preparation of chiral monoliths has been a challenging task but, Liu and co-workers developed relatively new method for carrying out separation by porous polymer monolithic columns of poly(4-vinylpyridine-co-ethylene dimethacrylate) (poly(VP-EDMA)). The chirality was induced into the monolith by incorporating chiral framework MOF $[Zn_2(bdc)(L\text{-}lac)(DMF)]\cdot(DMF)$ prepared from Zinc nitrate, L-lactic acid and bdc. While, monolithic column was incapable of separation of racemic mixtures, monolithic-chiral MOF columns proved out to be excellent for separation of enantiomers of (±)-methyl phenyl sulfoxide by nano-liquid chromatography.[77]

A SURMOF-templated approach has been developed by Zhang and co-workers for the designing and formulation of a homochiral-polymer thin film. The homochiral poly- L-dopa thin film formed by introduction of self-polymerizing L-dopa monomer into pores of achiral SURMOF and thereafter subjecting the SURMOF to UV irradiation followed by etching of SURMOF. Further, the enantioselective adsorption of the thin film was investigated by QCM and it was revealed that the homochiral poly-L–dopa thin film could selectively separate naproxen with ee 32%.[78]

5. Conclusions and Future Outlook

The chiral porous MOF materials have been extensively developed and shown their high feasibility in the enantioselective separation for a variety of racemic mixtures. The various synthesis approaches based on the direct and indirect methods have yielded a vast array of chiral frameworks yielding diverse functionalities. The highly ordered porous architectures, well-defined pore size and a high density of chiral recognition sites have led to highly efficient separation capabilities of the MOFs for enantiomeric mixtures. The progress in the direction of membrane based chiral separation has further broadened the scope of future industrial applicability, thereby establishing the foothold of MOFs as emerging platforms in enantioseparation.

Acknowledgements

We acknowledge the Robert A. Welch Foundation (B-0027) for financial support of this work.

References

[1] a) D. G. Blackmond, *Cold Spring Harbor Perspect. Biol.* **2010**, *2*, a002147-a002147; b) Y. Chen, W. Ma, *PLoS Comput. Biol.* **2020**, *16*, e1007592-e1007592.
[2] L. D. Barron, *Nature* **2007**, *446*, 505–506.
[3] M. E. Tiritan, M. Pinto, C. Fernandes, *Molecules* **2020**, *25*, 1713.
[4] a) J. McConathy, M. J. Owens, *Prim. Care Companion J. Clin. Psychiatry* **2003**, *5*, 70–73; b) C. Fanali, G. D'Orazio, A. Gentili, S. Fanali, *Molecules* **2019**, *24*, 1119.
[5] E. Tokunaga, T. Yamamoto, E. Ito, N. Shibata, *Sci. Rep.* **2018**, *8*, 17131.
[6] A. Berthod, in *Chiral Recognition in Separation Methods: Mechanisms and Applications* (Ed.: A. Berthod), Springer Berlin Heidelberg, Berlin, Heidelberg, **2010**, pp. 1–32.
[7] a) D. B. Carrão, I. S. Perovani, N. C. P. de Albuquerque, A. R. M. de Oliveira, *TrAC Trends Anal. Chem.* **2020**, *122*, 115719; b) Z. Wang, J. Ouyang, W. R. G. Baeyens, *J. Chromatogr. B* **2008**, *862*, 1–14; c) M. Fillet, P. Hubert, J. Crommen, *Electrophoresis* **1998**, *19*, 2834–2840.
[8] D. Wu, F. Pan, W. Tan, L. Gao, Y. Tao, Y. Kong, *J. Sep. Sci.* **2020**, *43*, 337–347.
[9] a) Y. Lu, H. Zhang, Y. Zhu, P. J. Marriott, H. Wang, *Adv. Funct. Mater.* **2021**,31, 2101335; b) J.-H. Zhang, S.-M. Xie, M. Zi, L.-M. Yuan, *J. Sep. Sci.* **2020**, *43*, 134–149; c) Z. Sun, J. Hou, L. Li, Z. Tang, *Coord. Chem. Rev.* **2020**, *425*, 213481.
[10] a) R.-G. Xiong, X.-Z. You, B. F. Abrahams, Z. Xue, C.-M. Che, *Angew. Chem. Int. Ed.* **2001**, *40*, 4422–4425; *Angew. Chem.* **2001**, *113*, 4554–4557; b) J. M. Castillo, T. J. H. Vlugt, D. Dubbeldam, S. Hamad, S. Calero, *J. Phys. Chem. C* **2010**, *114*, 22207–22213.
[11] G. Perot, M. Guisnet, *J. Mol. Catal.* **1990**, *61*, 173–196.
[12] H. Li, M. Eddaoudi, M. O'Keeffe, O. M. Yaghi, *Nature* **1999**, *402*, 276–279.
[13] a) H.-C. Zhou, J. R. Long, O. M. Yaghi, *Chem. Rev.* **2012**, *112*, 673–674; b) M. Safaei, M. M. Foroughi, N. Ebrahimpoor, S. Jahani, A. Omidi, M. Khatami, *TrAC Trends Anal. Chem.* **2019**, *118*, 401–425; c) S. Yuan, L. Feng, K. Wang, J. Pang, M. Bosch, C. Lollar, Y. Sun, J. Qin, X. Yang, P. Zhang, Q. Wang, L. Zou, Y. Zhang, L. Zhang, Y. Fang, J. Li, H.-C. Zhou, *Adv. Mater.* **2018**, *30*, 1704303; d) X. Zhang, Z. Chen, X. Liu, S. L. Hanna, X. Wang, R. Taheri-Ledari, A. Maleki, P. Li, O. K. Farha, *Chem. Soc. Rev.* **2020**, *49*, 7406–7427.
[14] a) H. Furukawa, K. E. Cordova, M. O'Keeffe, O. M. Yaghi, *Science* **2013**, *341*, 1230444; b) R. Ricco, C. Pfeiffer, K. Sumida, C. J. Sumby, P. Falcaro, S. Furukawa, N. R. Champness, C. J. Doonan, *CrystEngComm* **2016**, *18*, 6532–6542; c) Inamuddin, R. Boddula, M. I. Ahamed, A. M. Asiri, in *Applications of Metal–Organic Frameworks and Their Derived Materials*, 2020, pp. i–xvi.
[15] a) K. Biradha, C. Seward, M. J. Zaworotko, *Angew. Chem. Int. Ed.* **1999**, *38*, 492–495; *Angew. Chem.* **1999**, *111*, 584–587; b) S. Decurtins, H. W. Schmalle, P. Schneuwly, J. Ensling, P. Guetlich, *J. Am. Chem. Soc.* **1994**, *116*, 9521–9528; c) R. E. Norman, N. J. Rose, R. E. Stenkamp, *J. Chem. Soc. Dalton Trans.* **1987**, 2905–2910; d) J. D. Ranford, J. J. Vittal, D. Wu, *Angew. Chem. Int. Ed.* **1998**, *37*, 1114–1116; *Angew. Chem.* **1998**, *110*, 1159–1162.
[16] J. S. Seo, D. Whang, H. Lee, S. I. Jun, J. Oh, Y. J. Jeon, K. Kim, *Nature* **2000**, *404*, 982–986.
[17] a) J. Liu, S. Mukherjee, F. Wang, R. A. Fischer, J. Zhang, *Chem. Soc. Rev.* **2021**, *50*, 5706–5745; b) Y. Lu, H. Zhang, Y. Zhu, P. J. Marriott, H. Wang, *Adv. Funct. Mater.* **2021**, *31*, 2101335; c) Y. Liu, W. Xuan, Y. Cui, *Adv. Mater.* **2010**, *22*, 4112–4135; d) Z. Han, W. Shi, P. Cheng, *Chin. Chem. Lett.* **2018**, *29*, 819–822; e) H. S. Wang, J. P. Wei, *Nanoscale* **2015**, *7*, 11815–11832; f) M. Xue, B. Li, S. Qiu, B. Chen, *Mater. Today* **2016**, *19*, 503–515; g) P. Peluso, V. Mamane, S. Cossu, *J. Chromatogr. A* **2014**, *1363*, 11–26; h) K. K. Bisht, B. Parmar, Y. Rachuri, A. C. Kathalikattil, E. Suresh, *CrystEngComm* **2015**, *17*, 5341–5356; i) K. D. M. Harris, S. J. M. Thomas, *ChemCatChem* **2009**, *1*, 223–231; j) K. Kim, M. Banerjee, M. Yoon, S. Das, in *Functional Metal-*

Organic Frameworks: Gas Storage, Separation and Catalysis (Ed.: M. Schröder), Springer Berlin Heidelberg, Berlin, Heidelberg, **2010**, 115–153; k) C. Chang, X. Wang, Y. Bai, H. Liu, *TrAC Trends Anal. Chem.* **2012**, *39*, 195–206; l) W. Lin, *MRS Bull.* **2007**, *32*, 544–548; m) B. Kesanli, W. Lin, *Coord. Chem. Rev.* **2003**, *246*, 305–326.

[18] a) G. Nickerl, A. Henschel, R. Grünker, K. Gedrich, S. Kaskel, *Chem. Ing. Tech.* **2011**, *83*, 90–103; b) J.-H. Zhang, R.-Y. Nong, S.-M. Xie, B.-J. Wang, P. Ai, L.-M. Yuan, *Electrophoresis* **2017**, *38*, 2513–2520; c) T. Duerinck, J. F. M. Denayer, *Chem. Eng. Sci.* **2015**, *124*, 179–187.

[19] a) S.-Y. Zhang, D. Fairen-Jimenez, M. J. Zaworotko, *Angew. Chem. Int. Ed.* **2020**, *59*, 17600–17606; *Angew. Chem.* **2020**, *132*, 17753–17759; b) S. Das, S. Xu, T. Ben, S. Qiu, *Angew. Chem. Int. Ed.* **2018**, *57*, 8629–8633; *Angew. Chem.* **2018**, *130*, 8765–8769.

[20] J. Zhang, S. Chen, A. Zingiryan, X. Bu, *J. Am. Chem. Soc.* **2008**, *130*, 17246–17247.

[21] X. Zhao, E. T. Nguyen, A. N. Hong, P. Feng, X. Bu, *Angew. Chem. Int. Ed.* **2018**, *57*, 7101–7105; *Angew. Chem.* **2018**, *130*, 7219–7223.

[22] M. Zhang, X. D. Xue, J. H. Zhang, S. M. Xie, Y. Zhang, L. M. Yuan, *Anal. Methods* **2014**, *6*, 341–346.

[23] J. Wang, J. J. Chen, T. Y. Xu, *Solid State Sci.* **2019**, *98,* 106032.

[24] K. Cai, N. Zhao, N. Zhang, F.-X. Sun, Q. Zhao, G.-S. Zhu, *Nanomaterials* **2017**, *7*, 88.

[25] E. V. Anokhina, A. J. Jacobson, *J. Am. Chem. Soc.* **2004**, *126*, 3044–3045.

[26] E. V. Anokhina, Y. B. Go, Y. Lee, T. Vogt, A. J. Jacobson, *J. Am. Chem. Soc.* **2006**, *128*, 9957–9962.

[27] S. Wang, M. Wahiduzzaman, L. Davis, A. Tissot, W. Shepard, J. Marrot, C. Martineau-Corcos, D. Hamdane, G. Maurin, S. Devautour-Vinot, C. Serre, *Nat. Commun.* **2018**, *9*, 4937.

[28] H. T. Tang, K. K. Yang, K. Y. Wang, Q. Meng, F. Wu, Y. Fang, X. Wu, Y. G. Li, W. C. Zhang, Y. F. Luo, C. F. Zhu, H. C. Zhou, *Chem. Commun.* **2020**, *56*, 9016–9019.

[29] Q. Yue, W. X. Guo, Y. Y. Wang, X. L. Hu, E. Q. Gao, *Cryst. Growth Des.* **2019**, *19*, 2476–2484.

[30] a) G. Z. Yuan, H. Jiang, L. Y. Zhang, Y. Liu, Y. Cui, *Coord. Chem. Rev.* **2019**, *378*, 483–499; b) S. Bhattacharjee, M. I. Khan, X. F. Li, Q. L. Zhu, X. T. Wu, *Catalysts* **2018**, *8*, 120.

[31] a) C. Zhu, G. Yuan, X. Chen, Z. Yang, Y. Cui, *J. Am. Chem. Soc.* **2012**, *134*, 8058–8061; b) C. Baleizão, H. Garcia, *Chem. Rev.* **2006**, *106*, 3987–4043.

[32] S.-H. Cho, B. Ma, S. T. Nguyen, J. T. Hupp, T. E. Albrecht-Schmitt, *Chem. Commun.* **2006**, 2563–2565.

[33] Q. Xia, Z. Li, C. Tan, Y. Liu, W. Gong, Y. Cui, *J. Am. Chem. Soc.* **2017**, *139*, 8259–8266.

[34] J. Li, Y. Ren, C. Qi, H. Jiang, *Chem. Commun.* **2017**, *53*, 8223–8226.

[35] J. Bonnefoy, A. Legrand, E. A. Quadrelli, J. Canivet, D. Farrusseng, *J. Am. Chem. Soc.* **2015**, *137*, 9409–9416.

[36] C. Zhuo, F. Wang, J. Zhang, *CrystEngComm* **2018**, *20*, 5925–5928.

[37] D. Chen, R. Luo, M. Li, M. Wen, Y. Li, C. Chen, N. Zhang, *Chem. Commun.* **2017**, *53*, 10930–10933.

[38] X. Hou, T. Xu, Y. Wang, S. Liu, J. Tong, B. Liu, *ACS Appl. Mater. Interfaces* **2017**, *9*, 32264–32269.

[39] Z. Lin, A. M. Z. Slawin, R. E. Morris, *J. Am. Chem. Soc.* **2007**, *129*, 4880–4881.

[40] S.-Y. Zhang, D. Li, D. Guo, H. Zhang, W. Shi, P. Cheng, L. Wojtas, M. J. Zaworotko, *J. Am. Chem. Soc.* **2015**, *137*, 15406–15409.

[41] D. Wu, K. Zhou, J. Tian, C. Liu, J. Tian, F. Jiang, D. Yuan, J. Zhang, Q. Chen, M. Hong, *Angew. Chem. Int. Ed.* **2021**, *60*, 3087–3094; *Angew. Chem.* **2021**, *133*, 3124–3131.

[42] T. Ezuhara, K. Endo, Y. Aoyama, *J. Am. Chem. Soc.* **1999**, *121*, 3279–3283.

[43] R. Cui, H. Niu, E. Sheng, *Dalton Trans.* **2021**, *50*, 7186–7190.

[44] a) S. Shankar, R. Balgley, M. Lahav, R. Popovitz-Biro, S. R. Cohen, M. E. van der Boom, *J. Am. Chem. Soc.* **2015**, *137*, 226–231; b) M. C. di Gregorio, P. Ranjan, L. Houben, L. Shimon, K. Rehav, M. Lahav, M. E. van der Boom, *J. Am. Chem. Soc.* **2018**, *140*, 9132–9139; c) M. C. di Gregorio, L. Shimon, V. Brumfeld, L. Houben, M. Lahav, M. E. van der Boom, *Nat. Commun.* **2020**, *11*, 380; d) M. C. di Gregorio, M. Elsousou, Q. Wen, L. Shimon, V. Brumfeld, L. Houben, M. Lahav, M. E. van der Boom, *Nat. Commun.* **2021**, *12*, 957; e) Q. Wen, S. Tenenholtz, L. Shimon, O. Bar-Elli, L. Neeman, L. Houben, S. Cohen, Y. Feldman, D. Oron, M. Lahav, M. E. van der Boom, *J. Am. Chem. Soc.* **2020**, *142*, 1410–1422; f) V. Singh, L. Houben, L. Shimon, S. Cohen, O. Golani, Y. Feldman, M. Lahav, M. E. van der Boom, *Angew. Chem. Int. Ed.* **2021**, *60*, 2–11; *Angew. Chem.* **2021**, *133*, 2–2.

[45] M. C. Das, Q. S. Guo, Y. B. He, J. Kim, C. G. Zhao, K. L. Hong, S. C. Xiang, Z. J. Zhang, K. M. Thomas, R. Krishna, B. L. Chen, *J. Am. Chem. Soc.* **2012**, *134*, 8703–8710.

[46] W. M. Xuan, M. N. Zhang, Y. Liu, Z. J. Chen, Y. Cui, *J. Am. Chem. Soc.* **2012**, *134*, 6904–6907.

[47] H. X. Zhang, F. Wang, Y. X. Tan, Y. Kang, J. Zhang, *J. Mater. Chem.* **2012**, *22*, 16288–16292.

[48] Z. J. Li, J. Yao, Q. Tao, L. Jiang, T. B. Lu, *Inorg. Chem.* **2013**, *52*, 11694–11696.

[49] Y. A. Satska, N. P. Komarova, K. S. Gavrilenko, O. V. Manoylenko, Z. V. Chernenko, M. A. Kiskin, S. V. Kolotilov, I. L. Eremenko, V. M. Novotortsev, *Theor. Exp. Chem.* **2015**, *51*, 45–53.

[50] Z.-X. Xu, H.-R. Fu, X. Wu, Y. Kang, J. Zhang, *Chemistry* **2015**, *21*, 10236–10240.

[51] J. Liu, F. Wang, Q.-R. Ding, J. Zhang, J. Liu, *Inorg. Chem.* **2016**, *55*, 12520–12522.

[52] Y. A. Satska, E. A. Mikhalyova, Z. V. Chernenko, S. V. Kolotilov, M. Zeller, I. V. Komarov, A. V. Tymtsunik, A. Tolmachev, K. S. Gavrilenko, A. W. Addison, *RSC Adv.* **2016**, *6*, 93707–93714.

[53] Y. A. Satska, N. P. Komarova, K. S. Gavrilenko, R. A. Polunin, O. V. Manoylenko, S. V. Kolotilov, *Theor. Exp. Chem.* **2017**, *53*, 204–209.

[54] C. C. Zou, Q. Q. Li, F. J. Cheng, H. J. Wang, J. G. Duan, W. Q. Jin, *CrystEngComm* **2017**, *19*, 2718–2722.

[55] A. Abbas, Z. X. Wang, Z. J. Li, H. Jiang, Y. Liu, Y. Cui, *Inorg. Chem.* **2018**, *57*, 8697–8700.

[56] S. Das, S. X. Xu, T. Ben, S. L. Qiu, *Angew. Chem. Int. Ed.* **2018**, *57*, 8629–8633; *Angew. Chem.* **2018**, *130*, 8765–8769.

[57] Y. Z. H. Lu, J. Y. Chan, H. C. Zhang, X. Y. Li, Y. Nolvachai, P. J. Marriott, X. W. Zhang, G. P. Simon, M. M. B. Holl, H. T. Wang, *J. Membr. Sci.* **2021**, *620*, 118956.

[58] W. Wang, X. Dong, J. Nan, W. Jin, Z. Hu, Y. Chen, J. Jiang, *Chem. Commun.* **2012**, *48*, 7022–7024.

[59] M. Y. Li, F. Wang, J. Zhang, *Cryst. Growth Des.* **2020**, *20*, 5644–5647.

[60] D. Asnaghi, R. Corso, P. Larpent, I. Bassanetti, A. Jouaiti, N. Kyritsakas, A. Comotti, P. Sozzani, M. W. Hosseini, *Chem. Commun.* **2017**, *53*, 5740–5743.

[61] R. Bueno-Perez, A. Martin-Calvo, P. Gomez-Alvarez, J. J. Gutierrez-Sevillano, P. J. Merkling, T. J. H. Vlugt, T. S. van Erp, D. Dubbeldam, S. Calero, *Chem. Commun.* **2014**, *50*, 10849–10852.

[62] J. Zhao, H. Li, Y. Han, R. Li, X. Ding, X. Feng, B. Wang, *J. Mater. Chem. A* **2015**, *3*, 12145–12148.
[63] Y. Gao, W. R. Du, A. J. Yu, X. L. Li, W. D. Zhao, S. S. Zhang, *Anal. Methods* **2018**, *10*, 5811–5816.
[64] X. Bao, L. J. Broadbelt, R. Q. Snurr, *Mol. Simul.* **2009**, *35*, 50–59.
[65] Z. Long, J. Jia, S. L. Wang, L. Kou, X. D. Hou, M. J. Sepaniak, *Microchem. J.* **2013**, *110*, 764–769.
[66] X. Luo, Y. Cao, T. Wang, G. Li, Q. Huo, Y. Liu, J. Li, Y. Yang, Z. Xu, J. Zhang, M. Eddaoudi, *J. Am. Chem. Soc.* **2016**, *138*, 786–789.
[67] J. Y. Chan, H. Zhang, Y. Nolvachai, Y. Hu, H. Zhu, M. Forsyth, Q. Gu, D. E. Hoke, X. Zhang, P. J. Marriot, H. Wang, *Angew. Chem. Int. Ed.* **2018**, *57*, 17130–17134; *Angew. Chem.* **2018**, *130*, 17376–17380.
[68] K. Huang, X. L. Dong, R. F. Ren, W. Q. Jin, *AIChE J.* **2013**, *59*, 4364–4372.
[69] X. Lian, B. Yan, *ACS Appl. Mater. Interfaces* **2018**, *10*, 29779–29785.
[70] C. X. Tan, K. W. Yang, J. Q. Dong, Y. H. Liu, Y. Liu, J. W. Jiang, Y. Cui, *J. Am. Chem. Soc.* **2019**, *141*, 17685–17695.
[71] B. Liu, M. Tu, D. Zacher, R. A. Fischer, *Adv. Funct. Mater.* **2013**, *23*, 3790–3798.
[72] Z. G. Gu, S. Grosjean, S. Brase, C. Woll, L. Heinke, *Chem. Commun.* **2015**, *51*, 8998–9001.
[73] B. Liu, O. Shekhah, H. K. Arslan, J. X. Liu, C. Woll, R. A. Fischer, *Angew. Chem. Int. Ed.* **2012**, *51*, 807–810; *Angew. Chem.* **2012**, *124*, 831–835.
[74] D. Suttipat, S. Butcha, S. Assavapanumat, T. Maihom, B. Gupta, A. Perro, N. Sojic, A. Kuhn, C. Wattanakit, *ACS Appl. Mater. Interfaces* **2020**, *12*, 36548–36557.
[75] S. M. Chen, M. Liu, Z. G. Gu, W. Q. Fu, J. Zhang, *ACS Appl. Mater. Interfaces* **2016**, *8*, 27332–27338.
[76] Z. G. Gu, W. Q. Fu, X. Wu, J. Zhang, *Chem. Commun.* **2016**, *52*, 772–775.
[77] X. Wang, A. Lamprou, F. Svec, Y. Bai, H. W. Liu, *J. Sep. Sci.* **2016**, *39*, 4544–4548.
[78] Z. G. Gu, W. Q. Fu, M. Liu, J. Zhang, *Chem. Commun.* **2017**, *53*, 1470–1473.

Manuscript received: July 14, 2021
Revised manuscript received: August 29, 2021
Version of record online: September 29, 2021